2013-06-28

A Model for Sensory Neuron Development by FGF and Notch: A Multifactorial Approach

Jacob Eugene Voelkel
Brigham Young University - Provo

A Model for Sensory Neuron Development by FGF and Notch:

A Multifactorial Approach

Jacob E. Voelkel

A thesis submitted to the faculty of
Brigham Young University
in partial fulfillment of the requirements for the degree of

Master of Science

Michael Stark, Chair
Jeffery Barrow
R. Paul Evans

Department of Physiology and Developmental Biology

Brigham Young University

June 2013

ABSTRACT

A Model for Sensory Neuron Development by FGF and Notch:
A Multifactorial Approach

Jacob E. Voelkel

Physiology and Developmental Biology, BYU
Master of Science

The ophthalmic trigeminal placode (opV) exclusively gives rise to sensory neurons. A number of signaling pathways including Wnt, PDGF, FGF, and Notch are all involved in the progression of an undifferentiated cell in the opV placode to a proneural cell in the condensing opV ganglion. However, the regulatory relationships between these signal transduction pathways are still unknown. To determine if FGF activation acts to modulate Notch signaling in the sensory neurogenesis pathway, a novel multifactorial approach was employed: FGF signaling was inhibited in individual cells and globally with simultaneous inactivation of Notch signaling in chick embryos to investigate if FGF activation downregulates Notch thereby driving neurogenesis. These experiments resulted in few differentiating opV cells in the mesenchymal region of future ganglion formation suggesting an alternate regulatory relationship between FGF and Notch where either reduced Notch activity allows for FGFR4 expression (leading to FGF signaling and neurogenesis), or a parallel relationship where FGF and Notch act independently of one another to induce neurogenesis. To distinguish between these two possibilities Notch signaling was inhibited with DAPT, a gamma-secretase inhibitor, and assayed for FGFR4 mRNA expression. These results indicated FGFR4 is not upregulated by reduced Notch activity, suggesting that FGF and Notch act in parallel to promote neurogenesis. During these experiments it was observed that Notch inhibition resulted in an undefined ectoderm in the opV placode region. To investigate this, FGF and Notch were inhibited by SU5402, an FGF antagonist, and DAPT, and later sectioned and stained for Laminin. In DAPT treated embryos the basement membrane became highly fragmented, a remarkable observation not yet reported. From these data a proposed mechanism was established where activation of FGF with parallel downregulation of Notch leads to disruption of extracellular matrix proteins in the basement membrane resulting in fragmentation and subsequent delamination of differentiating opV placode cells.

Keywords: sensory neurogenesis, trigeminal ophthalmic placode, FGF signaling, Notch signaling, multifactorial

ACKNOWLEDGEMENTS

I would like thank Dr. Michael Stark for his time, guidance, counsel, and especially for his encouragement. He has pushed me to become a better student, researcher, and independent thinker.

I am also grateful to Dr. Jeffery Barrow for his optimistic attitude and for Dr. Paul Evans for his encouragement and support.

I appreciate all of the hard work the members of the Stark lab have contributed to this research and I am especially grateful for the guidance, counsel, time, and patience of Dr. Jason Adams and Dr. Rhonda Lassiter.

I would also like to thank my parents, Roger and Carol Voelkel for their positive influence and encouragement throughout this time and my loving wife, Tausha Voelkel, who has sacrificed much for me and who has always supported me.

TABLE OF CONTENTS

LIST OF TABLES

LIST OF FIGURES

INTRODUCTION

Sensory neurons send projections to the central nervous system in order to relay information from external stimuli. Understanding the development of such neurons would provide significant insight to the process of neurogenesis; undifferentiated ectoderm cells adopting neuronal cell fate. In addition, understanding normal neuronal differentiation is an important step in addressing diseases such as macular degeneration, glaucoma, hyperalgesia, and other sensory derived pathologies.

In vertebrates, areas of head ectoderm termed cranial placodes and a subset of neural crest cells give rise to all peripheral sensory neurons of the cranial ganglia (D'Amico-Martel and Node, 1983). Most neural precursor tissue can give rise to multiple cell types; however, the ophthalmic trigeminal placode (opV) exclusively differentiates into neurons within the trigeminal ganglion making it a unique model in the study of sensory neurogenesis (Begbie et al., 2002; Figure 1).

Since the discovery of Pax3 as an early marker of ophthalmic trigeminal placode cells (Stark et al. 1997) significant progress has been made in determining how these cells become specified and differentiate. One method of defining the developmental age of a vertebrate embryo is based on somite stage (ss). Induction of the opV placode begins with the expression of Pax3 at the 4 ss in chick. Induced cells become specified and committed by the 8 somite stage (Baker et al., 1999) and differentiate and delaminate at 13 and 18-26 ss respectively.

For the past decade, core publications have helped to characterize the function of genes known to be expressed in the opV placodes. Early studies showed that Wnt signaling is required for the initial development and maintenance of the otic placode (Ladher et al, 2000, 2005; Martin

and Groves, 2006; Ohyama et al., 2006). More recently, publications have shown that the functional genes Pax3 and FGFR4, as well as the canonical Wnt and Notch/Delta signaling pathways are all active during sensory neurogenesis in the opV placode (Lassiter et al., 2007, 2009, 2010; Canning et al., 2008; Dude et al., 2009).

Molecular pathways in sensory neurogenesis

Individual studies have shown that Wnt signaling is active in Pax3+ cells as early as the 3 ss and is necessary but not sufficient to induce sensory neuron formation in the opV placode on its own (Lassiter 2007). Dominant Negative Tcf4 (DN-Tcf) blocks Wnt signaling by acting as a constitutive repressor of canonical Wnt targets due to its inability to bind β-Catenin (Megason and McMahon, 2002). In Lassiter et al. 2007, it is shown that blocking canonical Wnt signaling via DN-Tcf inhibits the normal expression of opV placode markers including Pax3, FGFR4, and Eya 2 and disrupts delamination, neurofilament expression, and neuronal differentiation. This study further characterized the role of Wnt signaling in the opV placode by conducting misexpression experiments which did not result in expanded neuronal differentiation. Thus, it was concluded that Wnt signaling is necessary but not sufficient to induce Pax3 in competent ectoderm.

FGF signaling influences the development of the otic and lens placodes. Localized FGF signaling induces uncommitted ectoderm lateral to the developing hindbrain to develop the vertebrate inner ear (reviewed by Ohyama et al., 2006; Schimmang, 2007; Ladher et al., 2010). Disruption of FGF3 and FGF8 signaling by SU5402, an FGF receptor antagonist, blocks critical steps in the development of the otic placode. In Zebrafish it has also been shown that FGF signaling must be active through midsomitogenesis to maintain otic placode cell fate (Léger and

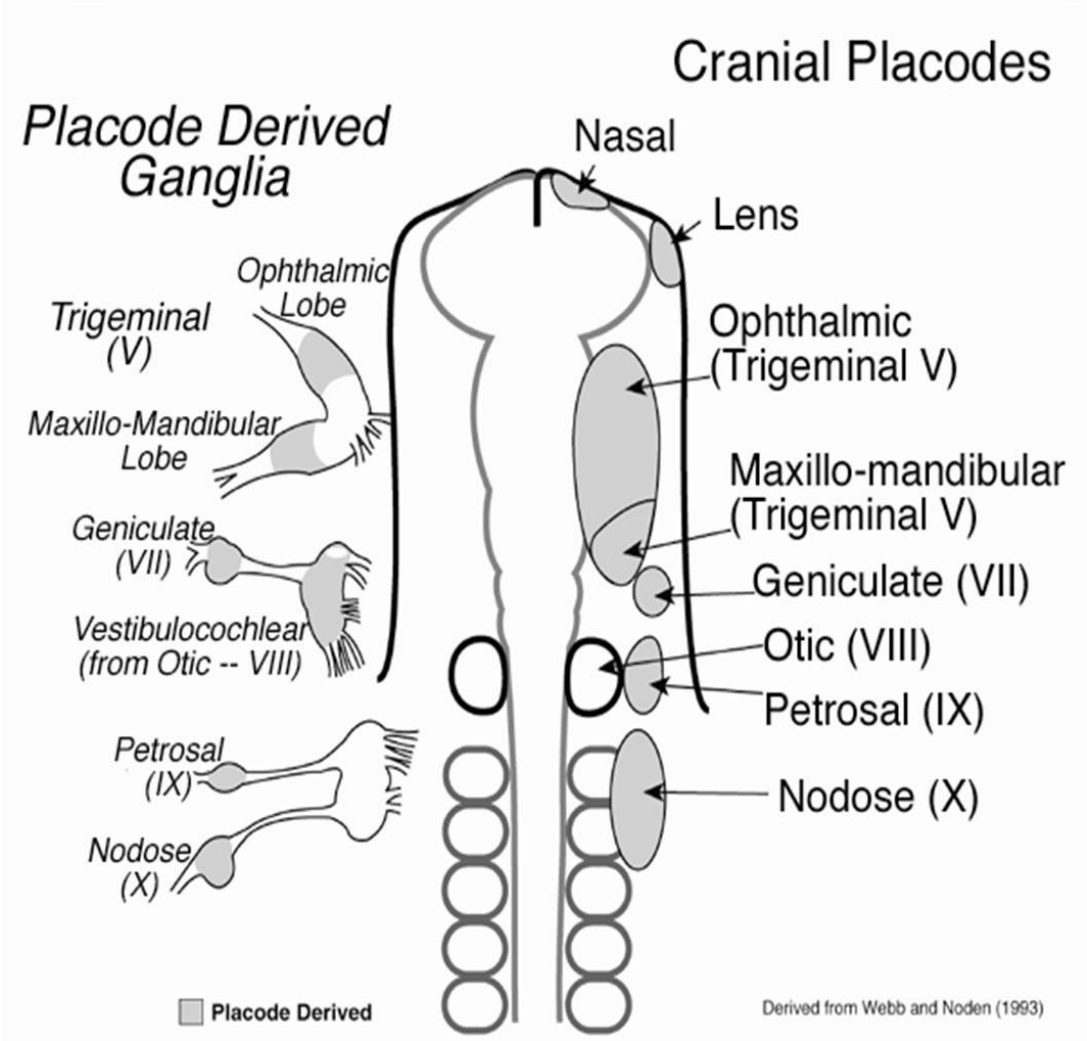

Figure 1 Neurogenic placodes of the head including the trigeminal placode made up of the ophthalmic and maxillo-mandibular regions.

Brand, 2002). Additionally, FGF signaling is required for the development of the lens placode in mice (Garcia et al., 2011). In chick, initial expression of FGFR4 mRNA in the opV placode domain occurs shortly after expression of Pax3 at the 10 ss. Individual opV placode cells express FGFR4 transiently with peak expression occurring just prior to and during epithelial-to-mesenchymal transition (EMT) at the 15-28 ss. FGFR4 expression is then quickly downregulated and is not detected in the condensing trigeminal ganglion (Stark et al., 1997). Studies in which FGF signaling was blocked with a secreted-FGFR4 (sFGFR4) showed Pax3 downregulation at 28 ss or within 30 hr after electroporation and that cell delamination from the placode to the spot of future ganglion formation was blocked, thus providing a role for FGF for delamination during sensory neurogenesis. However, misexpression studies failed to expand both Pax3+ placodal cells and delaminating cells (Lassiter et al., 2009).

In the Notch/Delta signaling pathway, a well-known regulator of cellular and neuronal differentiation, the transmembrane Notch receptor is activated by Delta or Serrate membrane bound ligands. The function of Notch signaling can be viewed as a switch that regulates developmental choices (Lewis, 1998). Many studies have characterized the general rule that precocious neuronal differentiation occurs when Notch signaling is blocked and neuronal cell fate is inhibited when Notch signaling is activated (Bolós et al., 2007; Yoon and Gaiano, 2005; Abelló et al., 2007; Daudet et al., 2007; Nelson et al., 2007; Kageyama et al., 2005; Lewis, 1998). In sensory neurogenesis reduced Notch signaling in the avian dorsal root ganglion resulted in the generation of DRG neurons while Notch activation prevented neuronal differentiation but permitted glial differentiation in vitro (Wakamatsu et al., 2000). A later study providing a spatiotemporal description the *Ngn2*, which induces the expression of Delta1 (Castro et al., 2006) and is inhibited by the Notch effecter gene *Hes1* (Shimojo et al., 2008), in the opV

placode determined that *Ngn2* is first expressed ~10-11 ss with more robust expression at ~16 ss. It also concluded that inhibition of the Notch pathway by the gamma-secretase inhibitor, DAPT, leads to premature neuronal differentiation and was identified as the primary regulator of sensory neuron cell fate (Lassiter et al., 2010). Although several components involved in sensory neurogenesis have been identified, a more complete regulatory model of trigeminal sensory neurogenesis, including how these pathways complement one another, has not been formed.

Pathway interactions in development

In the developmental context, cell fate is determined by the activation of target genes through signal transduction as a ligand binds its receptor. An organism utilizes multiple signal transduction pathways that work in coordination to achieve complex patterns of gene expression. For example, it has been known that Wnt, FGF, and Notch signaling contribute to somite segmentation (Goldbeter, 2007). More recent research has focused on determining how these pathways work in coordination during development thereby regulating somite formation periodicity through a molecular oscillator known as the segmentation clock. It has been suggested Notch signaling acts as a regulator switch in somite segmentation in the mouse because many of its target genes are cyclic and could therefore control the oscillator of the segmentation clock while FGF and Wnt signaling act upstream and/or parallel to this pathway (Gibb et al., 2010). Consistent with this theory, Notch knockout mice showed a complete disruption of somitogenesis (Ferjentsik et al., 2009). Further, evidence from mutant mice with disrupted FGF signaling resulted in a decrease of the Notch target *Lunatic Fringe* which suggests FGF at least in part regulates Notch signaling (Wahl et al., 2007). It has also been shown that Wnt signaling regulates the expression of Notch ligand Dll1 suggesting that Wnt signaling lies upstream of Notch (Hoffman et al., 2004). In contrast however, inhibition of Notch activity in

Zebrafish does not completely disrupt somite segmentation and therefore may be coordinated by a Notch independent oscillator while FGF target genes control oscillations (Lewis et al., 2009; Ozbudak et al., 2008; Kawamura et al., 2005). Additionally, FGF and Wnt have been shown to interact in this system, where Wnt signaling is required for the expression of FGF target genes in somite segmentation (Aulehla et al., 2003; Gibb et al., 2009). Although the complete regulatory mechanism for the somite segmentation clock is not complete, it is clear that a high degree of cross talk between the Wnt, FGF, and Notch signaling pathways exists.

Coordination of Notch and FGF in development and neurogenesis

In addition to the regulation of the vertebrate segmentation clock through interactions between Wnt, FGF, and Notch signaling, other studies have also began to elucidate how FGF and Notch signaling pathways work in concert to coordinate complex developmental patterns. In neuroepithelial precursor mouse cells it was shown that FGF acts upstream of Notch where FGF activates Notch signaling thereby inhibiting neuronal differentiation (Faux et al., 2001). In an evaluation of embryonic cortical surface area, Rash et al., 2011 showed that FGF lies upstream of Notch and in part regulates cortical neurogenesis. In contrast however, it has also been shown that activation of Notch signaling in NIH 3T3 cells suppresses FGF-dependent cellular transformation indicating that Notch may lie upstream of FGF in this developmental context or work through an autoregulatory mechanism (Small et al., 2003).

Project Aims

Results from these studies suggest that Notch and FGF interact in a variety of developmental contexts. As described, the mechanism of this interaction is dependent on the cell type and organism. As such, Notch and FGF may be acting in concert in the development of

sensory neurons in the trigeminal ganglion by one of three mechanisms. First, Notch may be acting as a regulatory switch where FGF downregulates Notch/Delta, allowing for neurogenesis to proceed. Second, reduced Notch activity may stimulate increased FGFR4 expression leading to FGF signaling and neurogenesis. Finally, FGF may be acting in parallel with Notch (i.e. both involved, but no cross-talk) to induce sensory neuron formation (Figure 2).

The purpose of this study was to determine the regulatory relationship of sensory neurogenesis in the trigeminal placode between the FGF and Notch signaling pathways. To do this, a novel approach was used that allowed for the manipulation of multiple signaling pathways simultaneously by combining well-established experimental approaches. In order to test FGFR4 activation leading to Notch inhibition, Notch signaling was blocked with the gamma-secretase inhibitor DAPT while simultaneously blocking FGF signaling by electroporation with sFGFR4 or with the FGF antagonist SU402. Effectively, if Notch is downstream of FGF signaling and FGF acts to downregulate the Notch system, then downregulation of Notch should promote neurogenesis even in the absence of FGF signaling. If neurogenesis is blocked however, this suggests that either Notch is regulating FGF signaling, or that the two pathways are acting in parallel with one another to regulate neurogenesis (Figure 2). To distinguish between these two relationships FGFR4 mRNA expression can be assayed after blocking the Notch signaling pathway for 4 and 12 hr. If Notch regulates FGF signaling, FGFR4 mRNA expression should be upregulated compared to controls. However, if expression is equal between experimental and control embryos, this provides evidence that FGF and Notch are working in parallel to promote neurogenesis.

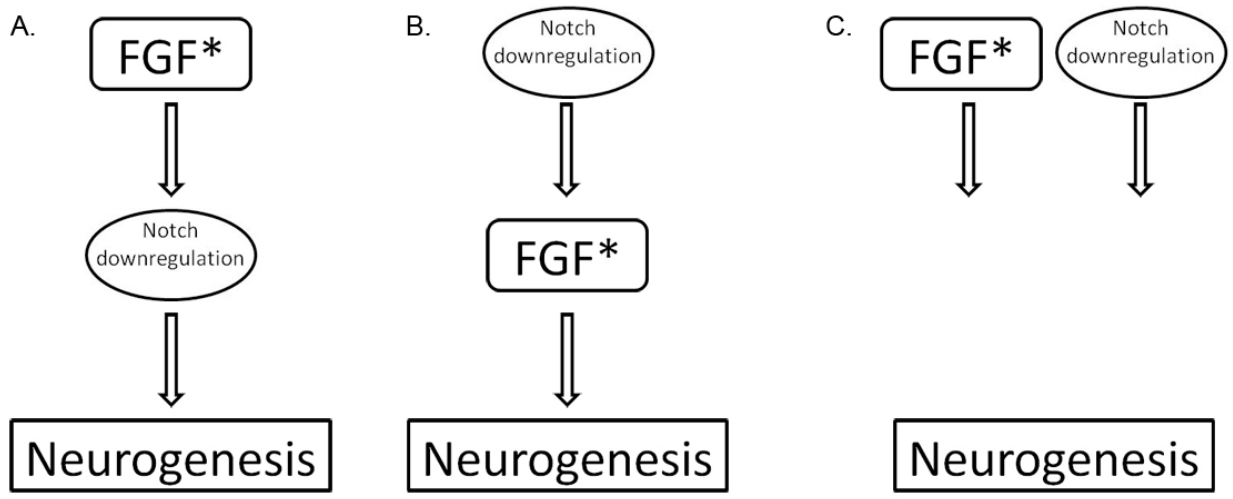

Figure 2 Proposed interactions of Fibroblast Growth Factor (FGF) and Notch signaling leading to Neurogenesis

(A) FGF activation downregulates Notch signaling leading to neurogenesis. In this model it would be expected that simultaneous inhibition of FGF and Notch would yield precocious neurogenesis by Notch downregulation overcoming FGF suppression.
(B) Notch downregulation leads to upregulation of FGFR4 expression and increased FGF signaling leading to neurogenesis. In this model it would be expected that simultaneous inhibition of FGF and Notch would cause cells to stall in the ectoderm terminating delamination and differentiation. In addition, Notch inhibition should lead to upregulation of FGFR4.
(C) FGF activation and Notch downregulation act in parallel to promote neurogenesis. In this model it would be expected that simultaneous inhibition of FGF and Notch would cause cells to stall in the ectoderm terminating delamination and differentiation. However, Notch inhibition would not lead to FGFR4 upregulation.
(*) Indicates activation of the pathway

MATERIALS AND METHODS

Preparation of Embryos

Fertilized chicken eggs (*Gallus gallus domesticus*, White Leghorn) from a local farm were incubated at 38^{o}C from 30-35 hr to the 6-9 or 12-14 somite stage. Once the embryos developed to the appropriate stage, the chick whole-embryo culture (Easy Chick, or EC) method developed by Susan Chapman et al., 2001 was used and adapted for these experiments. Each embryo was prepared by first cracking the egg into a Petri dish with the embryo facing up. The thick albumin surrounding the embryo was removed with a Kimwipe, and a ring of Whatman no.2 paper with an outer diameter of 1.0" and an inner diameter of 0.5" was placed around the embryo so that the embryo was in the center of the ring. Scissors were used to cut the vitelline membrane around the outside of the ring. Each embryo was then lifted with the ring, and briefly placed in Simple Saline to rinse away excess yolk. After the yolk was removed, a second ring was placed on the ventral side of the embryo creating a sandwich of two rings with the embryo and vitelline membranes in the center. The embryos were then electroporated in the ring or placed into agar-albumen culture dishes with the control or chemical inhibitor and incubated to an appropriate later stage. This technique was developed as a variation of the EC culture method allowing for subsequent removal of the cultured embryo onto a new media.

Agar-Albumen Culture Dishes with Chemical Inhibitor

Agar culture dishes are prepared according to Darnel and Schoenwolf (2000). 0.72 g of Bacto-Agar was mixed with boiling saline solution (7.19 g NaCl into 1L distilled water that has been autoclaved) and put in a water bath at 49^{o}C for 20 min. After twenty minutes the bacto agar/saline solution was removed from the water bath and mixed with thin albumin and 120 μL

of Penicillin/Streptomycin (10,000 units/mL) by swirling for 30-60 s in a flow hood. This solution was then mixed thoroughly with either 200 μM N-[N-(3,5-Difluorophenacetyl-L-alanyl)]-S-phenylglycine t-Butyl Ester (DAPT; EMD Chemicals Inc., Cincinnati, OH), 8 μL/mL of dimehtylsulfioxide (DMSO; Sigma-Aldrich Corp., St. Louis, MO), 50 μM SU5402, or 50 μM SU5402 plus 200 μM DAPT and placed in 6-welled dishes so that 2 mL of agar/chemical solution was in each well. Culture dishes were then covered and allowed to solidify for 3 hr to overnight at 4^{o}C prior to use.

Electroporation of sFGFR4 and pCIG in whole-embryo explants

The secreted quail FGF receptor-4 (sFGFR4) was ligated into the RSV/pCL vector with a separate SV40 promoter which drives Green Fluorescent Protein (GFP; Scaal et al., 2004). The sFGFR4 construct was a kind gift from Christophe Marcelle (Marics et al., 2002).

Electroporation with sFGFR4 DNA will block the FGF signaling pathway by expressing only the extracellular region of FGFR4; thereby binding ligand but not transducing any signal. Cells expressing the electroporated pCIG construct will report targeting as both the pCIG and sFGFR4 constructs have an attached GFP reporter. DNA constructs were prepared to a concentration of approximately 5 μg/μL in water with fast green added for visualization. An electrode was placed under the head of the chicken embryo and the DNA/fast green solution was applied over the trigeminal placode region with a micropipette. Another electrode used to drive the DNA into the cells was then placed above the head and seven pulses at 10ms each of 10 volts was applied by a BTX 820 electroporator (Gentronics). Following electroporation, the rings containing the embryo were placed in agar wells containing DMSO. After a period of four hr, sufficient time for the electroporated constructs to become expressed, the embryos were moved to an agar well containing DAPT and allowed to incubate at 37 °C for a total of 28 hr to the 24-

28 somite stage. After the incubation period each embryo was dissected from the ring, washed with phosphate-buffered saline (PBS), and fixed in 10 mL of 4% formaldehyde for one hr at room temperature or at 2-8^{o}C overnight. Following fixation, embryos were washed three times with PBS, placed in 5% sucrose/PBS for four hours at room temperature, and then stored in 15% sucrose/PBS at 2-8^{o}C until sectioning.

SU5402 and DAPT cultures

Embryos were grown to the 12-14 ss and prepared according to the modified EC culture method as described, placed on agar-albumin plates containing DMSO, SU5402, DAPT, or SU5402 plus DAPT, and incubated at 37^{o}C for 24 hr. Following the incubation period each embryo was dissected from the ring and prepared for cryosectioning in the same manner as electroporated embryos.

Cryosectioning and Immunohistochemistry

Embryos were prepared for cryosectioning by embedding them in gelatin consisting of 7.5 g gelatin (Sigma) and 15 g sucrose filled to a volume of 100 mL with 1xPBS. Each gelatin block was snap frozen in liquid nitrogen and sectioned at 12 μm with a cryostat and mounted on Superfrost® Plus glass slides. The gelatin surrounding the embryo sections was removed by placing slides in PBS at 25 ^{o}C for two 15 min washes and then for two additional five minute washes at 38^{o}C or until the gelatin dissolved and was no longer visible. The cryosections were then stained with primary antibodies.

The following primary antibodies were used: Pax3 (mouse IgG2a; Baker et al., 1999) and Islet-1 (mouse IgG2b; DSHB). Pax3 primary antibody was diluted to a 1:300 concentration with antibody buffer (PBS, 0.1%, bovine serum albumen (BSA), 0.1% Tween® 20) and Islet-1

primary antibody was diluted to a 1:200 concentration with antibody buffer. 300 µL of the primary antibody mixture was applied to each slide and allowed to incubate at 25 °C for four hours or at 4 °C for overnight. Each slide was then washed 3X 10 min with PBS, and then incubated with 300 µL of secondary antibody diluted in antibody buffer for one hour at 25 °C. Following application of the secondary antibody, the slides were washed twice with PBS for fifteen minutes each and covered using VWR micro cover glass 24 x 60 mm No.1 and several drops of Fluoromount-G. Fluorescent images of the staining were taken at 20X or 40X with an Olympus BX61 microscope.

In Situ Hybridization

Following culture with DAPT and incubation, experimental embryos undergoing *in situ* hybridization for FGFR4 mRNA expression were fixed in 4% formaldehyde for one hour at 25 °C. Following fixation, embryos were then washed three times for five minutes per wash in 1 mL Tween® 20 in 1L 1X PBS (PTW) and put sequentially into 25%, 50%, 75%, and 100% methanol in fifteen minute intervals and stored at -20 °C. Whole-mount *in situ* hybridization was then performed as described by Henrique et al., 1995. Briefly, formaldehyde-fixed embryos of appropriate developmental stages were buffered and exposed to a DIG-labeled anti-sense RNA probe which recognized the specific mRNA transcripts. After removal of the non-specifically adhering probe, the embryos were incubated with anti-DIG alkaline-phosphatase (AP) antibody (1/2000; Roche, Indianapolis, IN), followed by a chromogenic substrate for AP. Whole-mount embryos stained for specific mRNA transcripts and were then prepared for cryosectioning as described and sectional imaging was performed with brightfield microscopy.

Synthesis of the FGFR4 probe

A 400 bp fragment of chicken (*Gallus gallus*) *FGFR4* cDNA, corresponding to base-pairs 54–454 of chicken *FGFR4* (GenBank accession number AF083063), was PCR-amplified from a cDNA library of homogenised 3–10 somite-stage chick embryos using degenerate primers (5′-GGAGATGGAGCCAGACTCG-3′ and 5′-ACCTCTCCAGCACRTCCA-3′) and cloned into the pGEM-T easy vector (Promega).

Statistical Analysis

Cell counts were performed on randomly selected opV placodes using the Olympus Microsuite software (Olympus, Center Valley, PA). Cell counts for the electroporation experiments included cells expressing GFP, Islet1 antibody, and GFP and Islet1 antibody in the ectoderm and in the mesenchyme. Additional cell counts for SU5402+DAPT culture experiments included cells expressing Pax3 antibody, Islet1 antibody, and Pax3 and Islet1 antibody in the ectoderm and mesenchyme. Tukey-Kramer tests were performed using SAS software, version 9.2 (SAS Institute Inc., Cary, NC) to determine which means between experimental and control groups differed significantly in the analysis of variance. A p-value of ≤ 0.05 was considered statistically significant.

RESULTS

Inhibition of FGF and Notch signaling inhibits neurogenesis

Cells in the opV placode expressing sFGFR4 fail to delaminate and contribute to the ganglion (Lassiter et al., 2009). In contrast, inhibition of Notch in opV placode cells leads to premature neuronal differentiation with increased expression of the proneural marker Islet1 in the ectoderm and mesenchyme early in differentiation (Lassiter et al., 2010).To define the relationship between FGF and Notch signaling in opV neurogenesis, a multifactorial approach was used to simultaneously manipulate multiple signaling pathways.

In order to test whether FGFR4 activation acts to inhibit the Notch pathway, FGF signaling was blocked in 6-9 ss embryos via electroporation with secreted-FGFR4 (sFGFR4; Marics et al., 2002), which acts to inhibit FGF signaling by expressing only the extracellular domain (the first ~860 coding base pairs) of the molecule, thereby competing away endogenous FGF ligand. Targeted cells in experimental embryos electroporated with the sFGFR4 construct were identified by the expression of Green Fluorescent Protein (GFP) driven by a separate SV40 promoter within the sFGFR4 plasmid. Cells in control embryos electroporated with the pCIG construct were also identified by the expression of GFP driven by a promoter within the pCIG plasmid. Following electroporation, all embryos were allowed to incubate on an agar-albumen substrate with DMSO. After four hours, sufficient time for the electroporated construct to begin being expressed, Notch signaling was simultaneously blocked by transferring experimental embryos to an agar-albumin substrate containing 200 μM DAPT. All embryos were incubated and collected 24 hr later at the 24-28 ss. Experimental and control embryos were labeled as pCIG+DMSO, sFGFR4+DMSO, pCIG+DAPT and sFGFR4+DAPT.

After the embryos were cryosectioned through the opV placode/ganglion region they were stained with antibody as described. Using an Olympus BX61 Microscope, images of each of the sections were taken and saved to a database for analysis. A Random Number Generator program was used to randomly select up to five sections in the opV placode and the cellular effects of electroporated sFGFR4 and DAPT were quantified by counting the number of targeted opV cells that delaminated from cranial ectoderm and contributed to the opV ganglion. In all, the cells were counted as follows:

1. Total GFP+ cells in the mesenchyme
2. Total Islet1+ cells in the mesenchyme
3. Total GFP+/Islet1+ cells in the mesenchyme

It had been previously shown that Pax3 is downregulated in targeted cells (but apparently not in adjacent, untargeted cells) by the 28 somite stage, or within 30 hr after electroporation, in embryos electroporated with the sFGFR4 construct (Lassiter et al., 2009). Therefore, Pax3 was only minimally detectable in some targeted cells. This made it an unuseful marker for cell counts, but a valuable tool in identifying the opV placode/ganglion region.

Similar to results published in Lassiter et al., 2009, embryos electroporated with sFGFR4 and cultured in DMSO (sFGFR4+DMSO) showed a dramatic decrease in the number of GFP-labeled cells co-expressing the proneural marker Islet1 in the mesenchyme when compared with pCIG controls cultured in DMSO (Figure 3D,E,F). In sFGFR4+DMSO embryos (n = 7) no GFP+/Islet1+ cells were found contributing to the future opV ganglion in the mesenchyme (SEM ± 0.68) while embryos electroporated with pCIG and cultured in DMSO (pCIG+DMSO; n = 11) had an average of 3.3 GFP+/Islet1+ cells (SEM ± 0.56) per section. This experiment confirmed

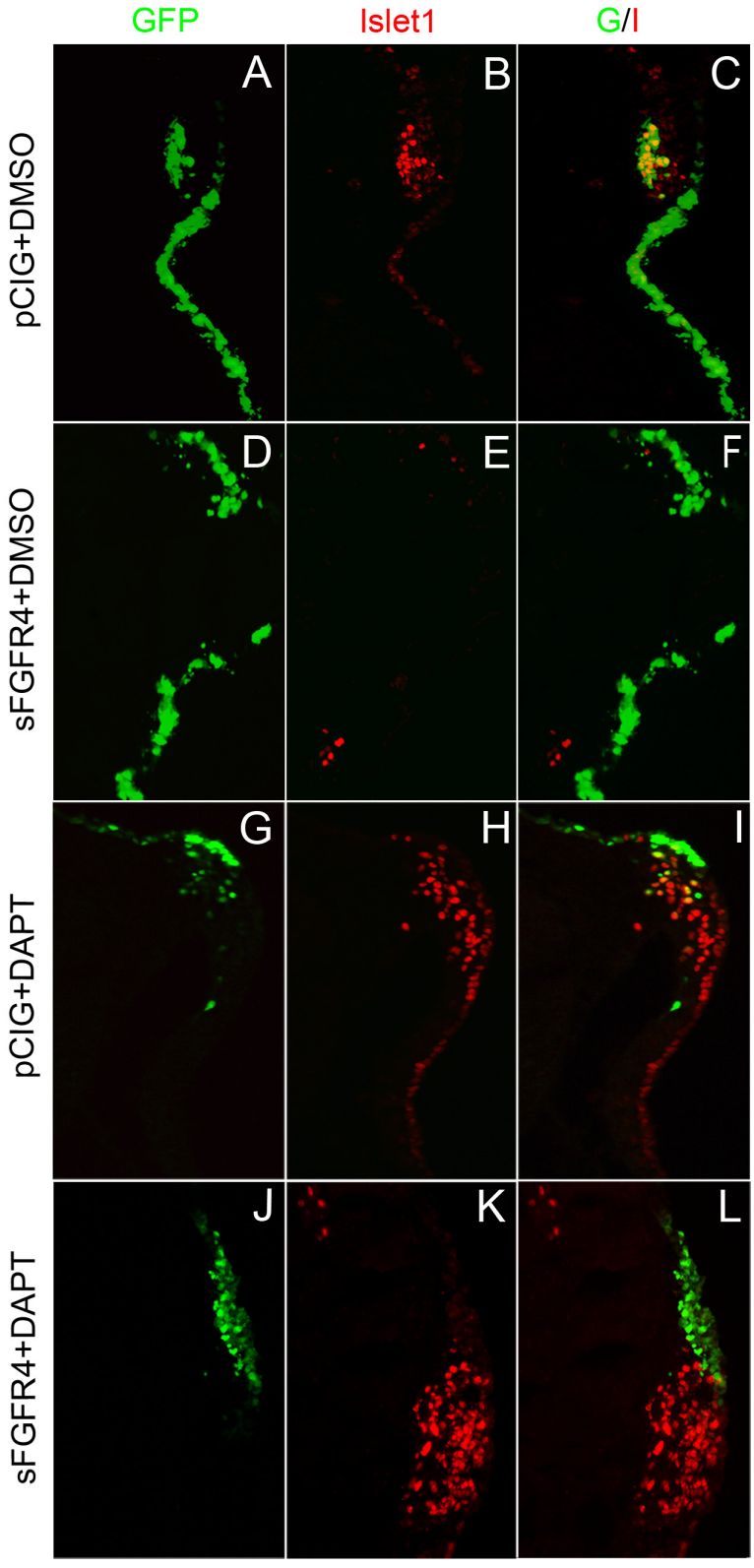

Figure 3 Notch inhibition cannot overcome FGF suppression to promote neurogenesis (legend on page 17)

Figure 3 Concurrent inhibition of fibroblast growth factor (FGF) and Notch signaling prevents targeted cells from differentiating, delaminating, and contributing to the ophthalmic trigeminal (opV) ganglion. A-L: Transverse section through the opV ganglion region of a ~24-28 somite stage (ss) embryo collected 28 hr after electroporation at the 6-9 ss with the control pCIG construct containing a green fluorescent protein (GFP) reporter and cultured with DMSO (A-C) or DAPT four hours after electroporation (G-I). Transverse sections through the opV ganglion of experimental embryos with secreted-FGFR4 misexpression construct (sFGFR4) cultured with DMSO (D-F) or DAPT (J-L) four hours after electroporation. GFP expression (green) marks targeted cells, with immunostaining for Islet1 (red; B,E,H,K). C: Merged image of GFP and Islet1; cells targeted with the pCIG construct with simultaneous treatment of DMSO migrate to the mesenchyme and coexpress the proneural marker Islet1. F: Merged imaged; GFP expressing cells targeted with sFGFR4 and treated with DMSO remain in ectoderm and do not express Islet1. I: Merged image; targeted pCIG GFP expressing cells treated with DAPT contribute substantially to the opV ganglion, with numerous cells co-expressing GFP and Islet1 (yellow) in the mesenchyme and a few co-expressing cells in the ectoderm. L: Merged image; GFP expressing cells targeted with sFGFR4 with concurrent DAPT treatment do not delaminate or express Islet1.

that blocking FGF signaling results in a significant decrease in cells differentiating in the mesenchyme when compared to controls ($p = 0.0012$; Table 1).

I also confirmed that cells targeted by electroporation with pCIG and cultured in DAPT (pCIG+DAPT) result in increased expression of the proneural marker Islet1 in the mesenchyme (Lassiter et al., 2010, Figure 3G,H,I). An average of 7.85 GFP+/Islet1+ cells (SEM ± 0.45) were found in the mesenchyme in pCIG+DAPT treated embryos ($n = 17$), a significant increase compared to the pCIG+DMSO controls ($p < 0.0001$, Table 1).

In order to determine the relationship between these findings a novel multifactorial approach was taken that allowed us to block the FGF and Notch signaling pathways simultaneously by electroporating with sFGFR4 and later culturing with DAPT (sFGFR4+DAPT). Quantitative analysis of these embryos showed an average of just 0.3 GFP+/Islet1+ cells in the mesenchyme (SEM ± 0.62) which was a significant decrease from pCIG+DMSO ($p = 0.002$) and pCIG+DAPT ($p < 0.0001$) treated embryos. Interestingly, the number of GFP+/Islet1+ cells in the mesenchyme of sFGFR4+DAPT treated embryos was not statistically different from sFGFR4+DMSO treated embryos ($p = 0.9880$; Figure 3J,H,L, Table 1).

Electroporating with sFGFR4 allowed individual cells to be analyzed to determine if cells could differentiate when FGF and Notch signaling was blocked. Results from these experiments indicate that inhibition of Notch and FGF signaling inhibits neurogenesis. If FGFR4 activation acts to inhibit Notch signaling, thereby allowing neurogenesis to proceed, it would have been expected that experimentally inhibiting Notch even with concurrent inhibition of FGF signaling would result in precocious neurogenesis. These results show that there is no statistical difference between embryos in which only FGF signaling is blocked and embryos in which FGF and Notch

signaling are simultaneously blocked. From this it can be concluded that FGF signaling acts in parallel with Notch to promote neurogenesis or that reduced Notch activity allows for FGF expression leading to neurogenesis (Figure 4).

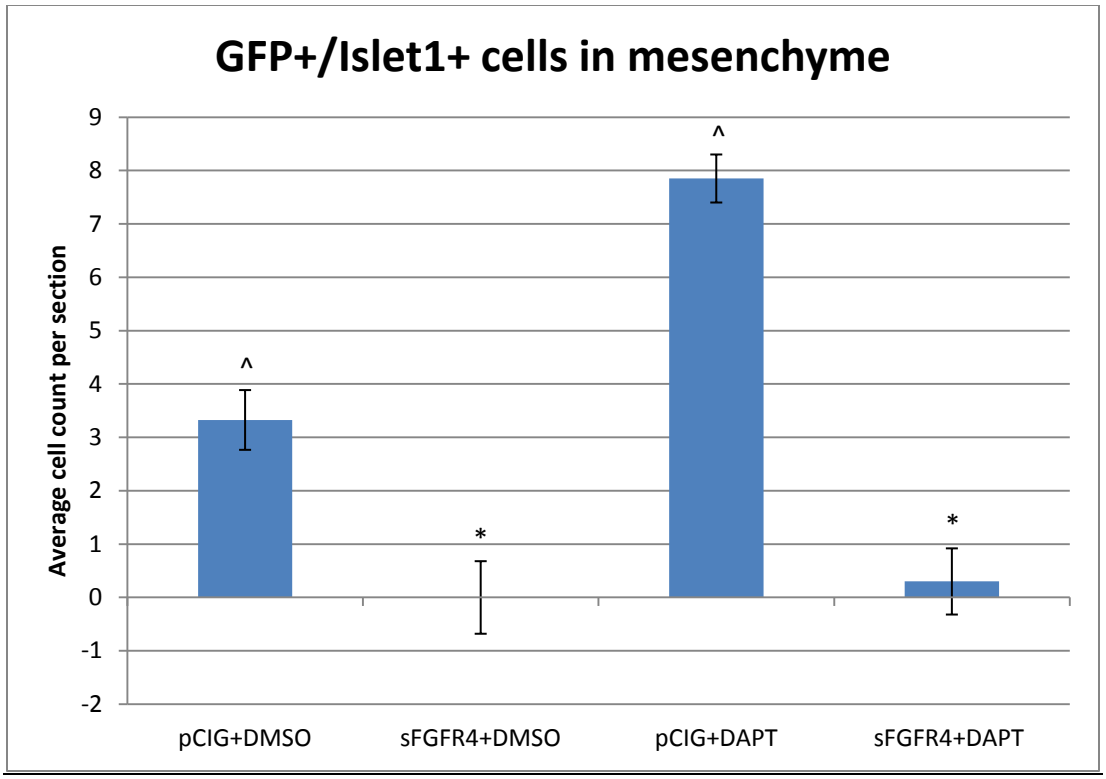

Figure 4 FGF inhibition combined with downregulation of Notch does not promote neurogenesis
Histogram describing GFP+/Islet1+ cells in the mesenchyme of embryos electroporated with pCIG or sFGFR4 with concurrent treatment of DMSO or DAPT. Control pCIG+DAPT and experimental sFGFR4+DAPT cell counts were from chick embryos electroporated at 6-9 ss and incubated on culture media containing 200 µM DAPT 4 hr after electroporation. Electroporated pCIG and sFGFR4 controls were cultured with 8 µL/mL of DMSO in agar-albumin substrate. All embryos were allowed to incubate until they reached the 24-28 ss before being collected. Targeted cells are reported via a GFP reporter attached to the pCIG and sFGFR4 constructs.
Error bars represent the standard error of the mean.
(*) p-value <0.05 between the experimental and control groups, pCIG + DAPT and pCIG + DMSO
(^) p-value <0.05 between the control groups pCIG + DAPT and pCIG + DMSO

Table 1

Misexpression construct ± culture treatment	Experiment number	Mean of the cell counts	Sample Size
pCIG + DMSO	1	3.33	11
sFGFR4+DMSO	2	0.00	7
pCIG + DAPT	3	7.85	17
sFGFR4 + DAPT	4	0.30	8

p-values	2	3	4
1	0.0012	<0.0001	0.0020
2		<0.0001	0.9880
3			<0.0001

Table 1 Tukey-Kramer analysis of GFP+/Islet1+ cells in the mesenchyme
6-9 ss embryos were electroporated with pCIG or sFGFR4 and cultured with DMSO or DAPT. Cells co-expressing GFP and Islet1 were counted in the mesenchyme of randomly selected opV placodes and a Tukey-Kramer analysis of cell counts was performed to show the statistical differences between experimental and control groups. The experimental groups with an assigned number, the mean of the cell counts for each experiment and sample size are all represented along with the associated p-values showing statistical differences between experimental groups.

Global inhibition of FGF and Notch signaling inhibits neurogenesis

Prior experiments employed the use of the FGF inhibitor SU5402 to determine the role of FGF signaling in the opV placode. By globally blocking FGF signaling, experimental outcome is not dependent on electroporation efficiency and allows for the evaluation of all potential opV sensory neurons. To test global inhibition of FGF embryos were grown to the 12-14 ss, prepared as described and incubated in agar wells containing either DMSO, 50 μM SU5402, 200 μM DAPT, or a combination of 50 μM SU5402 plus 200 μM DAPT (SU5402+DAPT) and allowed to incubate for 24 hr to the 24-28 ss. (12-14 ss embryos were used to ensure inhibition of FGF and Notch at a similar somite stage as electroporated embryos for comparison of the results.) Following incubation embryos were collected and prepared for immunohistochemistry as described and imaged using an Olympus BX61 Microscope. A Random Number Generator program was again used to select up to five sections through each opV placode/ganglion for analysis. For this experiment the following cells counts were collected:

1. Total Pax3+ cells in the mesenchyme
2. Total Islet1+ cells in the mesenchyme
3. Total Pax3+/Islet1+ cells in the mesenchyme

As described, Pax3 expression is downregulated by 28 ss in embryos electroporated with the sFGFR4 construct. However, in embryos treated with SU5402, Pax3 expression is maintained, although at weaker levels than in control embryos. Therefore, in these experiments Pax3 expression was used as a marker for the opV placode/ganglion and Pax3+/Islet1+ cells were analyzed.

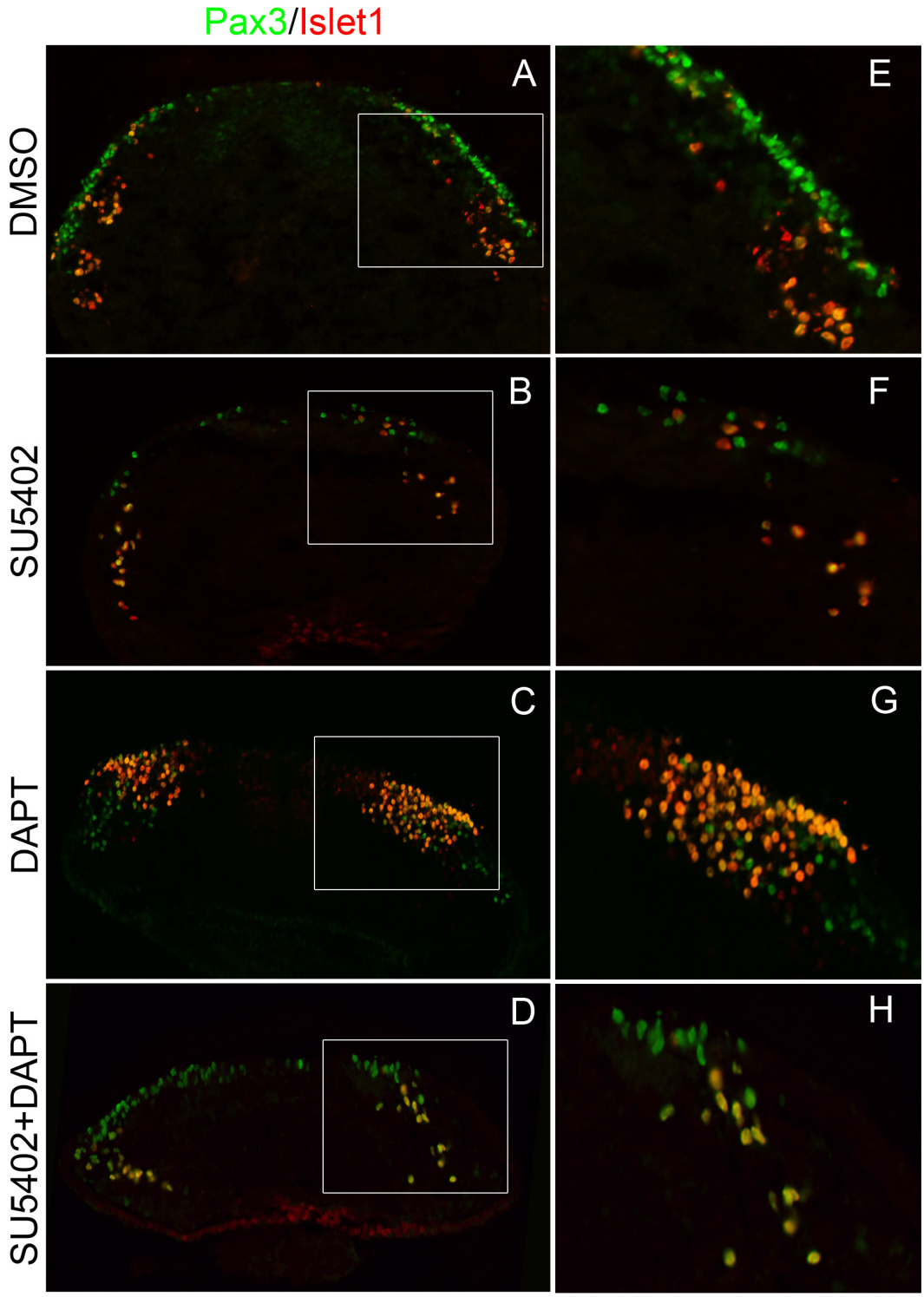

Figure 5 Global suppression of FGF and Notch inhibits delamination and differentiation (legend on page 24)

Figure 5 Transverse sections through the ophthalmic trigeminal (opV) placode region of 24-28 ss embryos cultured in DMSO, SU5402, DAPT, or SU5402 plus DAPT for 24 hr in agar-albumin culture dishes. (A-D) Embryos were prepared as described, cryosectioned, and immunostained for the opV marker Pax3 (green) and the early neuronal marker Islet1 (red). A magnified image is depicted in E-H. SU5402 treated embryos showed reduced Pax3+/Islet1+ cells in the mesenchyme (B,F) while DAPT treated embryos showed a dramatic increase in Pax3+/Islet1+ cells in the mesenchyme and premature neuronal differentiation in the ectoderm (C,G). Embryos treated with SU5402 and DAPT showed a significant reduction of cells co-expressing Pax3 and Islet1 in the mesenchyme compared to DMSO controls (D,H,). Interestingly, no difference was found between SU5402 and SU5402+DAPT treated embryos (Figure 6, Table 2).

Embryos treated with SU5402 revealed a significant decrease in the average number of Pax3+/Islet1+ mesenchyme cells per section (8.35; SEM ± 2.34; n = 4) when compared with DMSO controls (17.1; SEM ± 2.34; n = 5), a difference of 14.76 cells/placode (P = 0.0489). This data is comparable with results obtained in a previous study that characterized the effect of SU5402 on head explant cultures in the opV placode domain (Lassiter et al., 2009).

In embryos where Notch signaling was blocked, robust neuronal differentiation occurred. DAPT treated embryos had an average of 47.1 cells/section with co-localization of Pax3 and Islet1 (SEM ± 3.31; n = 2) in the mesenchyme; a significant increase from DMSO controls ($p < 0.0001$). Nearly all Pax3+ cells also co-expressed Islet1, an interesting result also noted by Lassiter et al., 2010.

To analyze dual inhibition of FGF and Notch globally both pathways were blocked simultaneously with SU5402 and DAPT (SU5402+DAPT). Remarkably, the combined treatment greatly reduced the average number of co-expressing Pax3 and Islet1 cells in the mesenchyme (8.8; SEM ± 2.10) compared to DAPT and DMSO controls ($p < 0.0001$, $p = 0.0489$). However, there was no statistical difference when compared to SU5402 treated embryos ($p = 0.9989$; Figure 6; Table 2).

This data corroborates the sFGFR4 electroporation results, where neurogenesis is significantly reduced. Taken together, these findings strongly suggest that Notch repression is unable to overcome FGF inhibition which suggests Notch may not act as a final switch promoting sensory neurogenesis in the opV placode.

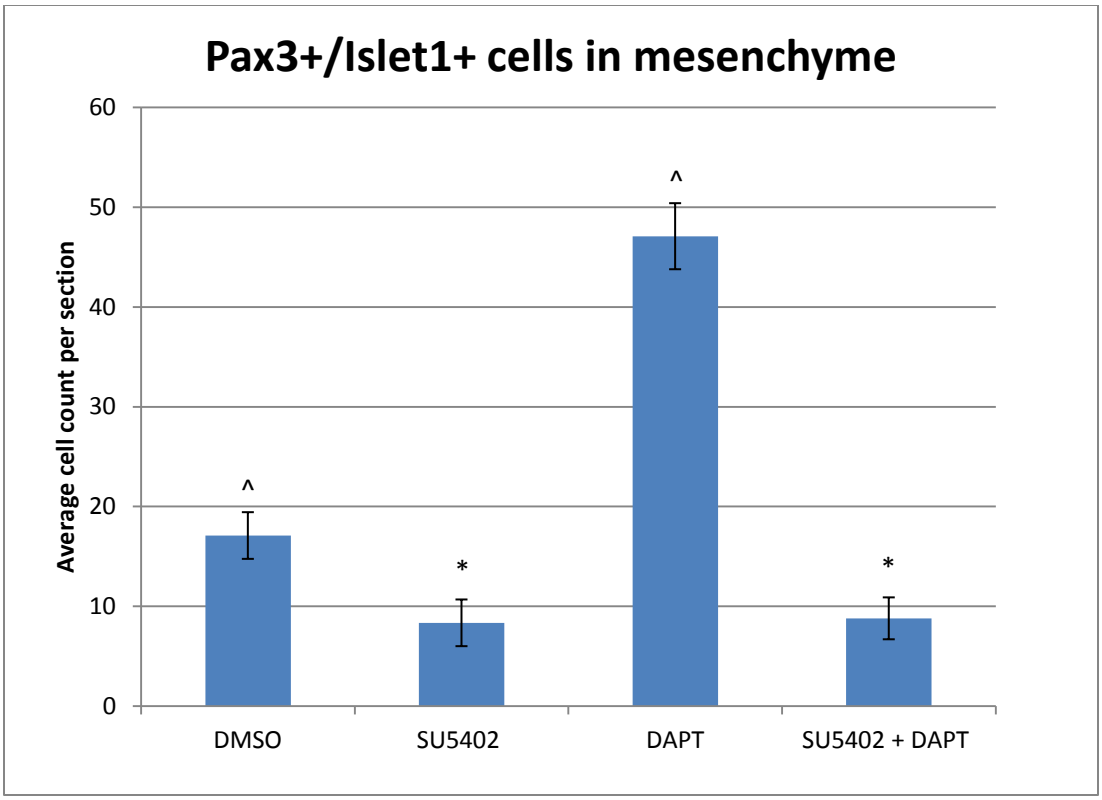

Figure 6 Inhibition of FGF and Notch leads to reduced neurogenesis in the mesenchyme
Histogram describing cells co-expressing Pax3 and Isle1 in the mesenchyme of 12-14 ss embryos treated with 8 µL/mL of DMSO in agar-albumin substrate, 50 µM SU5402, 200 µM DAPT, or 50 µM SU5402 plus 200 µM DAPT and incubated for 24 hr to the 24-28 ss.
Error bars represent the standard error of the mean.
(*) p-value <0.05 between SU5402 and SU5402+DAPT treated embryos and controls groups DMSO and DAPT
(^) p-value <0.05 between controls groups DMSO and DAPT

Table 2

Culture treatment	Experiment number	Mean of the cell counts	Sample Size
DMSO	1	17.10	4
SU5402	2	8.35	4
DAPT	3	47.18	2
SU5402 + DAPT	4	8.80	5

p-values	2	3	4
1	0.0489	<0.0001	0.0489
2		<0.0001	0.9989
3			<0.0001

Table 2 Tukey-Kramer analysis of Pax3/Islet1 expressing cells in the mesenchyme
12-14 ss embryos were incubated in agar-albumin culture dishes with DMSO, SU5402, DAPT, or SU5402+DAPT for 24 hrs. Following incubation, they were prepared as described, cryosectioned and immunostained. A Tukey-Kramer analysis of cell counts from random sections was performed to show the statistical differences between experimental and control groups. The experimental groups with an assigned number, the mean of the cell counts for each experiment and sample size are all represented along with the associated p-values showing statistical differences between experimental groups.

FGFR4 does not respond to inhibition of Notch signaling

Since FGF inhibition resulted in reduced neurogenesis even with simultaneous inhibition of Notch, the hypothesis that FGF activation leads to downregulation of Notch signaling to promote neurogenesis is false. Next, the hypothesis that Notch inhibition leads to upregulation of FGFR4 expression was tested. To do this, FGFR4 mRNA expression was assessed after blocking the Notch pathway with DAPT. FGFR4 mRNA expression within the opV placode domain initially occurs shortly after Pax3 expression, but is quickly downregulated and again is expressed prior to delamination. Therefore, 6-9 ss embryos were prepared as described and treated with 200 μM DAPT for 4 or 12 hr (Stark et al., 1997; Lassiter et al., 2009). Following DAPT treatment mRNA expression was analyzed by *in situ* hybridization. Results showed DAPT treated embryos expressed similar patterns of FGFR4 mRNA expression after 4 and 12 hr compared to DMSO treated controls (Figure 7,8). These results suggest that FGFR4 expression is not a direct target of Notch signaling modulation and that Notch signaling pathways work in parallel to promote neurogenesis in the opV ganglion.

If reduced Notch activity allows for FGFR4 expression and FGF signaling, inhibition of Notch by DAPT would be expected to upregulate FGFR4 mRNA expression in the opV placode. Since FGFR4 was not upregulated in experimental embryos, this suggests that FGF and Notch signaling do not regulate one another in opV placode cells and are each necessary but not sufficient to promote neurogenesis in the ophthalmic trigeminal ganglion.

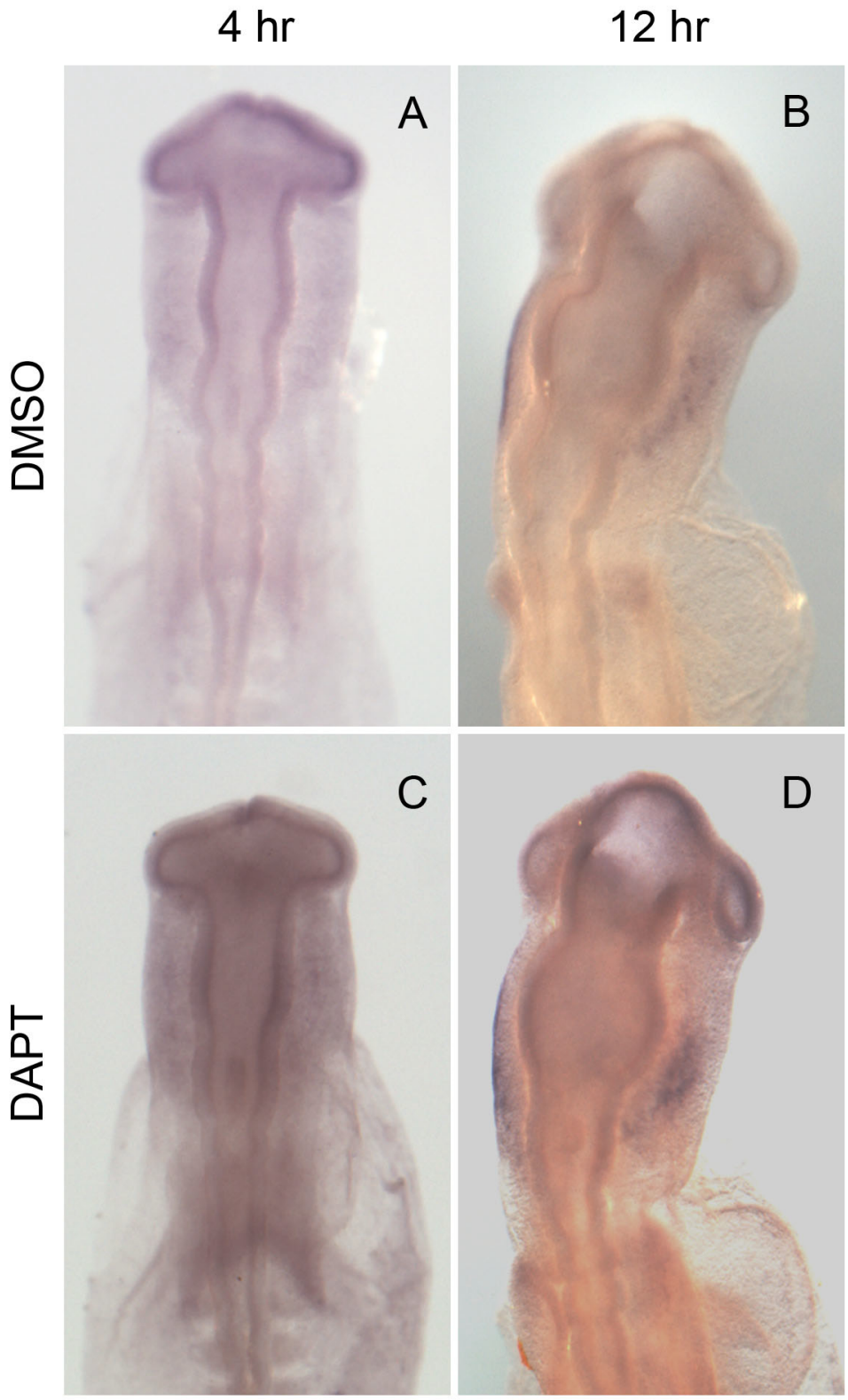

Figure 7 FGFR4 mRNA is not upregulated by Notch inhibition after 4 and 12 hr (legend on page 31)

Figure 7 6-9 ss embryos were incubated on agar-albumin dishes with 200 μM DAPT or DMSO, collected and prepared for *in situ* hybridization as described. FGFR4 mRNA expression was assayed after 4 and 12 hr due to the transient nature of FGFR4 expression. Increased levels of FGFR4 mRNA was observed after 12 hr in both DMSO and DAPT treated embryos (C,D) compared to levels observed after 4 hr of treatment (A,B). However, levels in experimental embryos were not observed to be significantly increased when compared to controls.

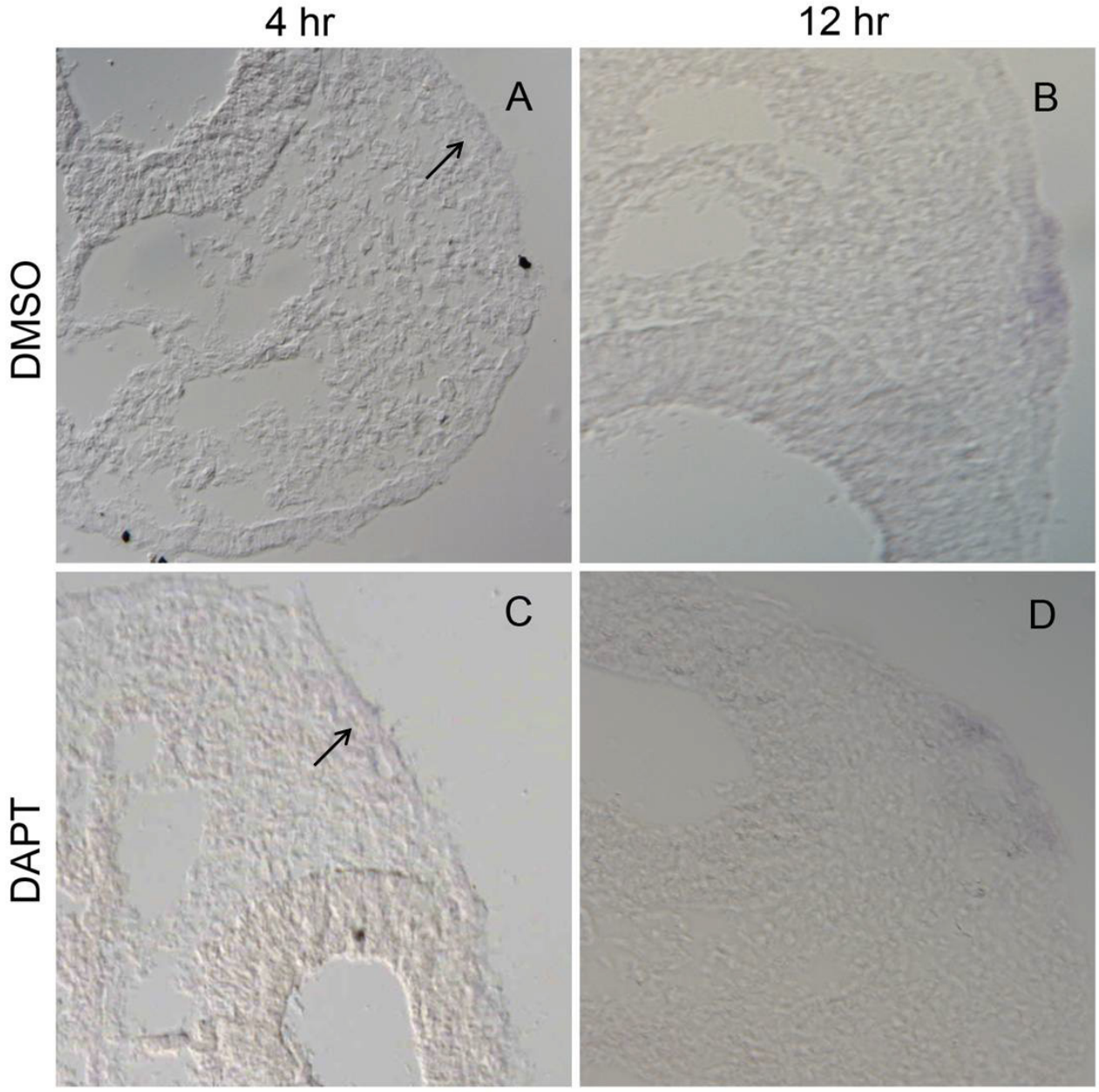

Figure 8 FGFR4 mRNA expression in transverse sections through the opV placode (figure legend on page 33)

Figure 8 6-9 ss embryos were incubated on agar-albumin dishes with 200 μM DAPT or DMSO, collected and prepared for *in situ* hybridization as described. Embryos were then prepared for cryosectioning and imaged using brightfield microscopy. FGFR4 mRNA expression was assayed after 4 and 12 hr due to the transient nature of FGFR4 expression.
No difference in FGFR4 mRNA expression was observed between experimental and control embryos after culture with DAPT for 4 or 12 hr.
(*) Arrow depicts FGFR4 mRNA

Simultaneous inhibition of FGF and Notch causes cells to stall in the ectoderm reducing delamination and differentiation

While previous studies have characterized the differentiation of ectoderm cells in the trigeminal placode after blocking the FGF or Notch pathways individually, I aimed to evaluate the effects of concurrent inhibition of the pathways. To test this, 6-9 ss embryos were electroporated with sFGFR4 and cultured in DMSO or DAPT and collected at the 24-28 ss. Control embryos (pCIG+DMSO or DAPT) were also generated. Following cryosectioning and immunostaining, sections from the opV placode were identified based on morphology and Pax3 expressing cells in the area. Images were obtained using an Olympus BX61 Microscope. The following cell counts were analyzed:

1. Total GFP+ cells in the ectoderm
2. Total Islet1+ cells in the ectoderm
3. Total GFP+/Islet1+ cells in the ectoderm

Again, because Pax3 is downregulated by the 28 somite stage, or within 30 hr after electroporation with the sFGFR4 construct (Lassiter et al., 2009), Pax3 was a used to identify the opV placode/ganglion region but not for cell counts

In order to test the effects of FGF and Notch co-inhibition on cells in the opV placode, I first blocked each pathway individually and compared these results to published data from Lassiter et al., 2009, which found that cells expressing the sFGFR4 construct in the ectoderm rarely co-expressed Islet1 24 hr after electroporation and did not express Islet1 36 hr after electroporation. Results showed that pCIG+DMSO treated embryos contained significantly fewer GFP expressing cells/section in the opV placode (17.5, SEM ± 1.48) when compared with sFGFR4+DMSO treated embryos (24.85, SEM ± 1.80; $p = 0.0055$; Figure 10, Table 4).

However, total GFP+ cells/section in the ectoderm plus mesenchyme were not significantly different (pCIG+DMSO, 23.29 ± 1.73 vs. sFGFR4+DMSO, 25.27 ± 2.10; $p = 0.8847$; Figure 9; Table 3). Most GFP+ cells in the ectoderm of sFGFR4+DMSO and pCIG+DMSO treated embryos did not co-express Islet1 (0.90, SEM ± 0.25; 0.52, SEM ± 0.31; Figure 11; Table 5). Similar to results published in Lassiter et al., 2009, these data suggest that cells expressing the sFGFR4 construct do not delaminate and do not contribute to ganglion formation (Figure 3A-F).

While embryos electroporated with sFGFR4 and treated with DMSO failed to delaminate and differentiate, embryos electroporated with pCIG and treated with DAPT showed significantly more cells/section co-expressing GFP and Islet1 in the ectoderm vs. pCIG+DMSO controls ($p = 0.0003$; normalized for total GFP+ cells), but no difference in total ectodermal GFP+ cells ($p = 0.9900$). Compared to sFGFR4+DMSO treated embryos, pCIG+DAPT treated embryos contained significantly fewer GFP+ cells in the ectoderm ($p = 0.0055$). These findings support data reported in Lassiter et al., 2010 and suggests that Notch inhibition by DAPT causes cells to undergo premature differentiation in the ectoderm while not affecting cellular delamination.

If blocking FGF inhibits delamination and differentiation in the opV placode and Notch downregulation promotes premature differentiation in the opV placode, what is the effect on the development of ectoderm cells in the opV placode when blocking both pathways simultaneously? To evaluate this question, 6-9 ss embryos were electroporated with sFGFR4 and transferred from an albumin-agar substrate containing DMSO to an albumin-agar substrate containing DAPT after four hr. Results showed that there was a significant reduction of co-expressing GFP and Islet1 cells in the ectoderm when compared to pCIG+DAPT control embryos ($p < 0.0001$). As with GFP+ cells in sFGFR4+DMSO treated embryos, GFP+ cells in

sFGFR4+DAPT treated embryos remained in the ectoderm and failed to delaminate. These data provide further evidence that cells expressing sFGFR4 stall in the ectoderm and fail to differentiate even in the presence of Notch downregulation by DAPT. This suggests FGF does not reduce Notch activity leading to differentiation in the ectoderm and that Notch inhibition cannot overcome suppression of FGF signaling to drive neurogenesis.

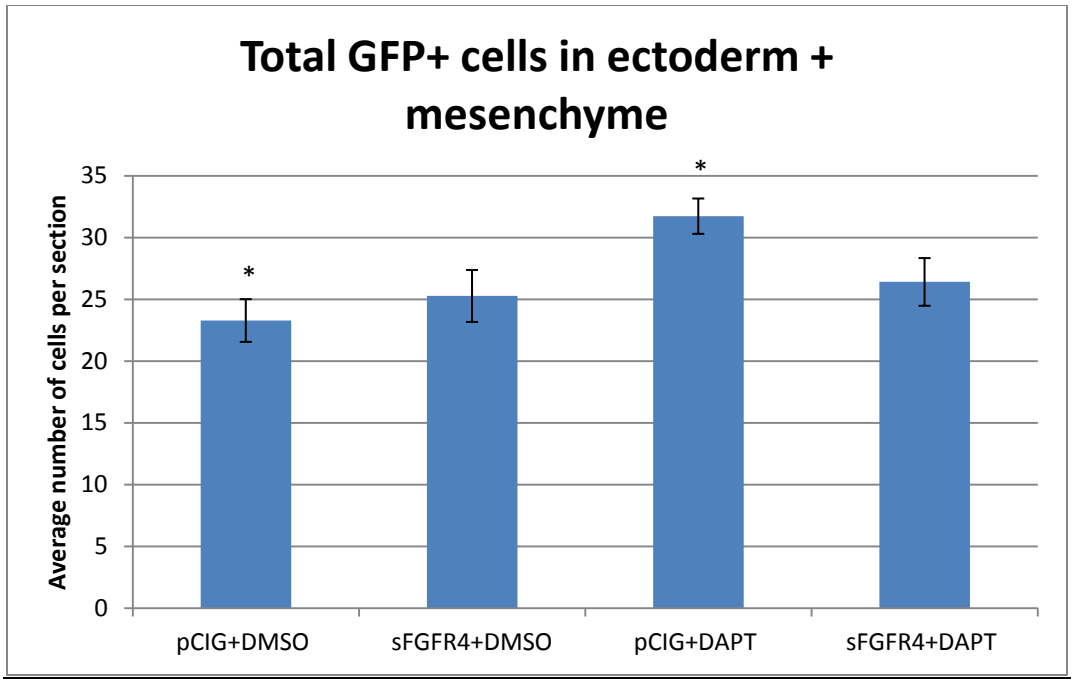

Figure 9 Total GFP expressing cells in the ectoderm plus mesenchyme
Histogram describing the total number of targeted cells in the ectoderm and mesenchyme of ~24-28 ss embryos electroporated with the pCIG control construct or sFGFR4 experimental construct at the 6-9 ss. Targeted cells were identified by a GFP reporter attached the electroporated constructs.
Error bars represent the standard error of the mean.
(*) p-value <0.05 between pCIG+DAPT treated embryos and pCIG+DMSO controls. No other statistical differences were observed (Table 3).

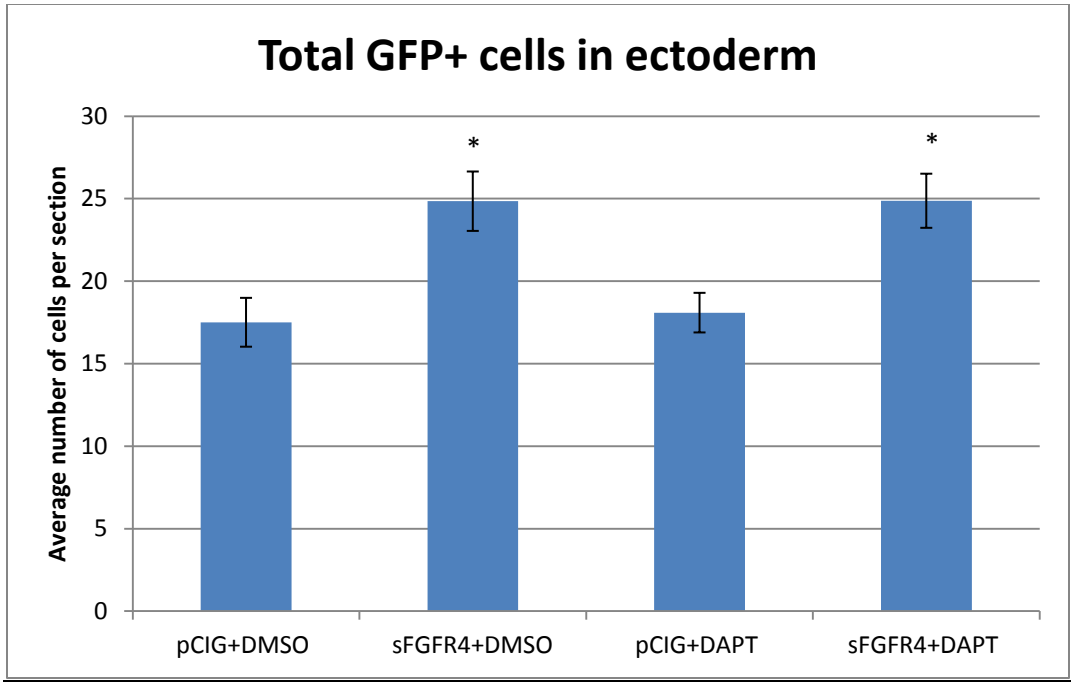

Figure 10 Cells expressing the sFGFR4 construct stall in the ectoderm and fail to delaminate even in the presence of DAPT

Histogram describing the total number of targeted cells remaining in the ectoderm of ~24-28 ss embryos electroporated with the pCIG control or sFGFR4 experimental construct at the 6-9 ss. Targeted cells were identified by a GFP reporter attached to each construct. Of interest, GFP expressing cells in sFGFR4+DMSO and sFGFR4+DAPT treated embryos stalled in the ectoderm and failed to contribute to ganglion formation.

Error bars represent the standard error of the mean.

(*) p-value <0.05 between sFGFR4+DMSO and sFGFR4+DAPT experimental embryos vs. control groups, pCIG+DMSO and pCIG+DAPT (Table 4)

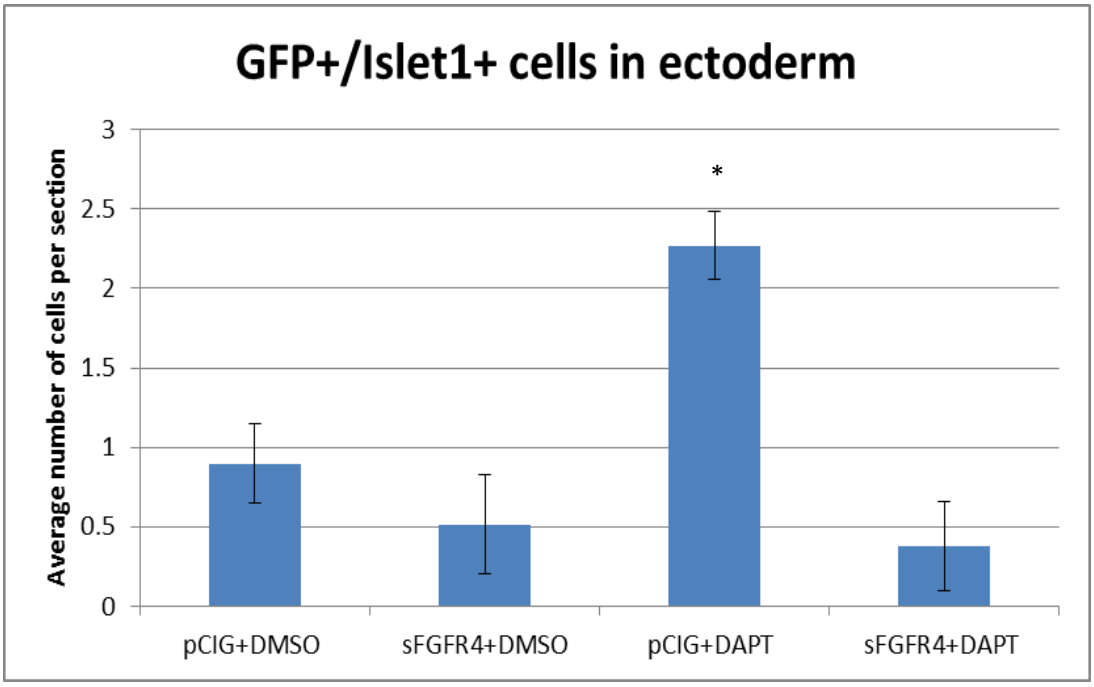

Figure 11 Notch downregulation cannot overcome FGF inhibition to promote premature neuronal differentiation in the ectoderm

Histogram describing cells co-expressing GFP and Islet1 in the ectoderm of ~24-28 ss embryos. 6-9 ss embryos were electroporated with pCIG or sFGFR4 and incubated in agar-albumin wells. After four hours embryos were either transferred to agar-albumin wells containing DAPT or remained in wells treated with DMSO and allowed to incubate for an additional 24 hr. Interestingly, it was observed that cells expressing sFGFR4 and treated with DAPT did not undergo premature neuronal differentiation in the ectoderm.

Error bars represent the standard error of the mean.

(*) p-value <0.05 between the pCIG+DAPT control group and pCIG+DMSO, sFGFR4+DMSO, and sFGFR4+DAPT (Table 5)

Table 3

Misexpression construct ± culture treatment	Experiment number	Mean of the cell counts	Sample Size
pCIG + DMSO	1	23.28	11
sFGFR4+DMSO	2	25.27	7
pCIG + DAPT	3	31.73	17
sFGFR4 + DAPT	4	26.41	8

p-values	2	3	4
1	0.8847	0.0013	0.6239
2		0.0573	0.9785
3			0.1239

Table 3 Tukey-Kramer analysis of total GFP expressing cells in the ectoderm and mesenchyme of ~24-28 ss embryos
6-9 ss embryos were electroporation with pCIG or sFGFR4 and cultured with DMSO or DAPT for 24 hr as described. Targeted cells expressing the GFP reporter were counted in the ectoderm and mesenchyme of randomly selected opV placodes and a Tukey-Kramer analysis of cell counts was performed to show the statistical differences between experimental and control groups. The experimental groups with an assigned number, the mean of the cell counts for each experiment and sample size are all represented along with the associated p-values showing statistical differences between experimental groups.

Table 4

Misexpression construct ± culture treatment	Experiment number	Mean of the cell counts	Sample Size
pCIG + DMSO	1	17.51	11
sFGFR4+DMSO	2	24.85	7
pCIG + DAPT	3	18.09	17
sFGFR4 + DAPT	4	24.88	8

p-values	2	3	4
1	0.0102	0.9900	0.0055
2		0.0112	1.0000
3			0.0055

Table 4 Tukey-Kramer analysis of GFP expressing cells in the ectoderm of ~24-28 ss embryos
6-9 ss embryos were electroporation with pCIG or sFGFR4 and cultured with DMSO or DAPT for 24 hr as described. Targeted cells expressing the GFP reporter were counted in the ectoderm and mesenchyme of randomly selected opV placodes and a Tukey-Kramer analysis of cell counts was performed to show the statistical differences between experimental and control groups. The experimental groups with an assigned number, the mean of the cell counts for each experiment and sample size are all represented along with the associated p-values showing statistical differences between experimental groups.

Table 5

Misexpression construct ± culture treatment	Experiment number	Mean of the cell counts	Sample Size
pCIG + DMSO	1	0.90	11
sFGFR4+DMSO	2	0.52	7
pCIG + DAPT	3	2.27	17
sFGFR4 + DAPT	4	0.38	8

p-values	2	3	4
1	0.7761	0.0003	0.5159
2		<0.0001	0.9871
3			<0.0001

Table 5 Tukey-Kramer analysis of cells co-expressing GFP and Islet1 in the ectoderm of ~24-28 ss embryos

6-9 ss embryos were electroporation with pCIG or sFGFR4 and cultured with DMSO or DAPT for 24 hr as described. Targeted cells expressing the GFP reporter were counted in the ectoderm and mesenchyme of randomly selected opV placodes and a Tukey-Kramer analysis of cell counts was performed to show the statistical differences between experimental and control groups. The experimental groups with an assigned number, the mean of the cell counts for each experiment and sample size are all represented along with the associated p-values showing statistical differences between experimental groups.

Global inhibition of FGF and Notch does not lead to premature differentiation in the ectoderm

Embryos electroporated with sFGFR4 helped characterize the effect of dual inhibition of FGF and Notch in individual ectoderm cells. To analyze inhibition of FGF and Notch on all potential opV sensory neurons, global inhibition of the pathways was accessed. To do this, embryos were grown to the 12-14 ss and treated with DMSO, 50 μM SU5402, 200 μM DAPT, or a combination of 50 μM SU5402 plus 200 μM DAPT (SU5402+DAPT) in an agar-albumin substrate and allowed to incubate for 24 hr. Following incubation, embryos were collected, cryosectioned, and prepared for immunostaining with Pax3 and Islet1. After imaging with an Olympus BX61 Microscope, random sections were selected and the following cells counts were performed:

1. Total Pax3+ cells in the ectoderm
2. Total Islet1+ cells in the ectoderm
3. Total Pax3+/Islet1+ cells in the ectoderm

As described, embryos treated with SU5402 contribute significantly fewer differentiating cells to ganglion formation compared to controls (Figure 5B,F; Table 2). Analysis of ectoderm cells in the opV placode treated with SU5402 revealed few co-expressing Pax3/Islet1 cells/section similar to controls (1.25 SEM ± 0.71 vs. 2.55 SEM ± 0.71; $p = 0.5747$; Table 6). This, along with evidence from the electroporation experiments, confirms the conclusion in Lassiter et al. (2009) that reduced FGF signaling inhibits delamination causing cells to remain in the ectoderm. Here, it is also show that these cells abandon their path towards neurogenesis and fail to differentiate in the ectoderm.

In concurrence with Lassiter et al. 2010, DAPT treated embryos contained significantly more Pax3+/Islet1+ cells in the ectoderm compared to controls (Figure 5C,G; Table 6).

However, global inhibition of FGF with SU5402 and Notch with DAPT resulted in few co-expressing Pax3 and Islet1 cells in the ectoderm not statistically different from DMSO or SU5402 treated embryos. Thus dual inhibition of FGF and Notch reversed the effect seen with DAPT treatment alone (Figure 5E,H; Table 6). As with results obtained from the sFGFR4 electroporation experiments, these results suggest that proneural ectoderm cells in the opV placode are not driven towards neurogenesis by FGF activation inhibiting Notch activity. Interestingly, few ectoderm cells express Islet 1 in control embryos and in embryos in which the FGF pathway is blocked by sFGFR4 misexpression or by SU5402 inhibition with or without concurrent inhibition of Notch by DAPT. In all cases however, significantly more cells express Islet1 when only the Notch pathway is inhibited (Figure 12).

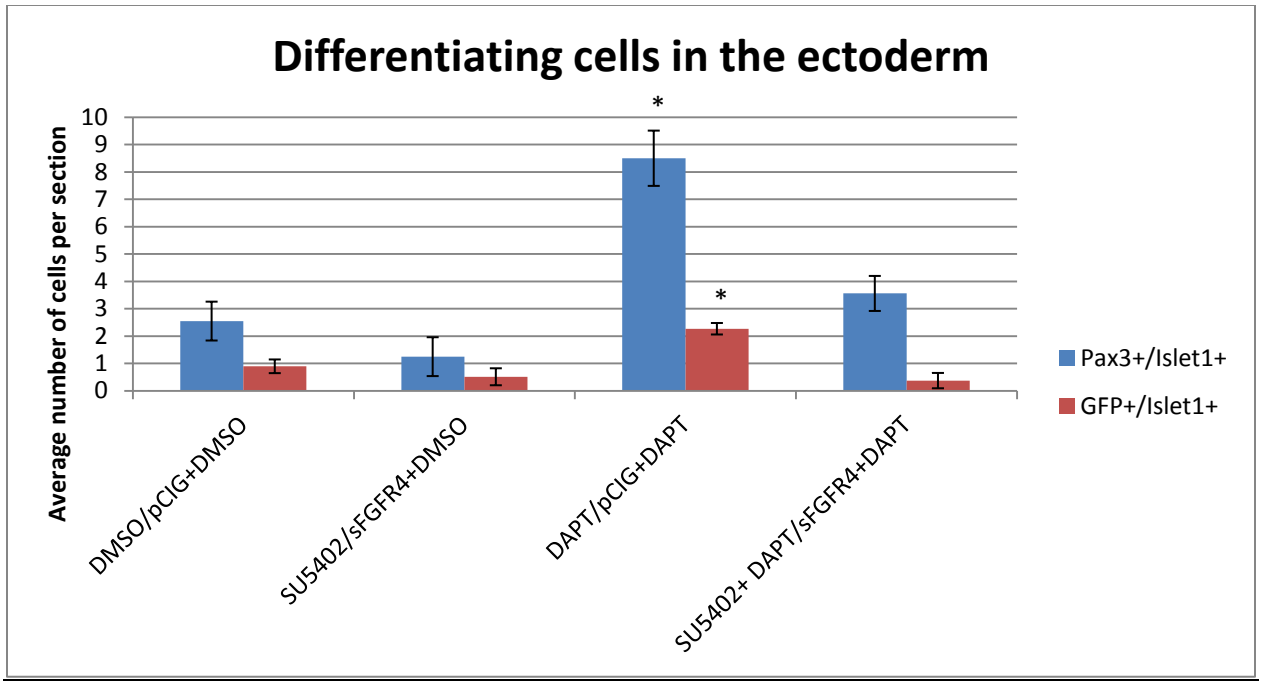

Figure 12 Blocking FGF globally or in individual cells with concurrent inhibition of Notch inhibits neurogenesis

Histogram describing cells co-expressing Pax3 and Islet1 in the ectoderm of 12-14 ss embryos treated with 8 µL/mL DMSO, 50 µM SU5402, 200 µM DAPT, or 50 µM SU5402 plus 200 µM DAPT and incubated for 24 hr to the 24-28 ss (blue) compared to cells co-expressing GFP and Islet1 as described in figure 8 (red). Of interest, globally blocking FGF results in the same statistical differences between experimental and control groups as sFGFR4 misexpression experiments with concurrent inhibition of Notch by DAPT.

Error bars represent the standard error of the mean.

(*) p-value <0.05 between DAPT treated embryos and DMSO, SU5402, and SU5402+DAPT treated embryos (Table 2)

Table 6

Culture treatment	Experiment number	Mean of the cell counts	Sample Size
DMSO	1	2.55	4
SU5402	2	1.25	4
DAPT	3	8.50	2
SU5402 + DAPT	4	3.56	5

p-values	2	3	4
1	0.5747	<0.0001	0.7188
2		<0.0001	0.0845
3			0.0006

Table 6 Tukey-Kramer analysis of Pax3/Islet1 expressing cells in the ectoderm
12-14 ss embryos were incubated in agar-albumin culture dishes with DMSO, SU5402, DAPT, or SU5402+DAPT for 24 hr. After incubation they were prepared as described, cryosectioned and immunostained. A Tukey-Kramer analysis of cell counts from random sections was performed to show the statistical differences between experimental and control groups. The experimental groups with an assigned number, the mean of the cell counts for each experiment and sample size are all represented along with the associated p-values showing statistical differences between experimental groups.

Activated FGF signaling coupled with Notch inhibition disrupts basement membrane integrity

Analysis of embryos treated with DAPT revealed an undefined ectoderm in the opV region when compared to controls. A similar observation was made in Lassiter et al., 2010. Because of growing interest in understanding tissue specific signals that regulate epithelial-mesenchymal transition (EMT), this was further investigated by determining the effects of FGF and Notch signaling on basement membrane integrity. To do this, 12-14 ss embryos were treated with DMSO, SU5402, DAPT, or SU5402 plus DAPT and incubated on agar-albumin culture as previously described. After 24 hr embryos were prepared, cryosectioned, and immunostained for Pax3, Islet1, and Laminin (Figure 13).

It was found that embryos treated with DAPT contained widely fragmented basement membrane in the placode region when compared to DMSO controls, as assayed by Laminin staining (Figure 13B, F). Embryos treated with SU5402 and SU5402+DAPT also contained areas of basement membrane disruption but not to the extent as seen in DAPT treated embryos. This finding suggests FGF activation and Notch downregulation results in changes that disrupt basement membrane integrity in the opV placode. To my knowledge this is the first time such data has been reported and with further investigation may provide further insight to the mechanisms of EMT in the opV region.

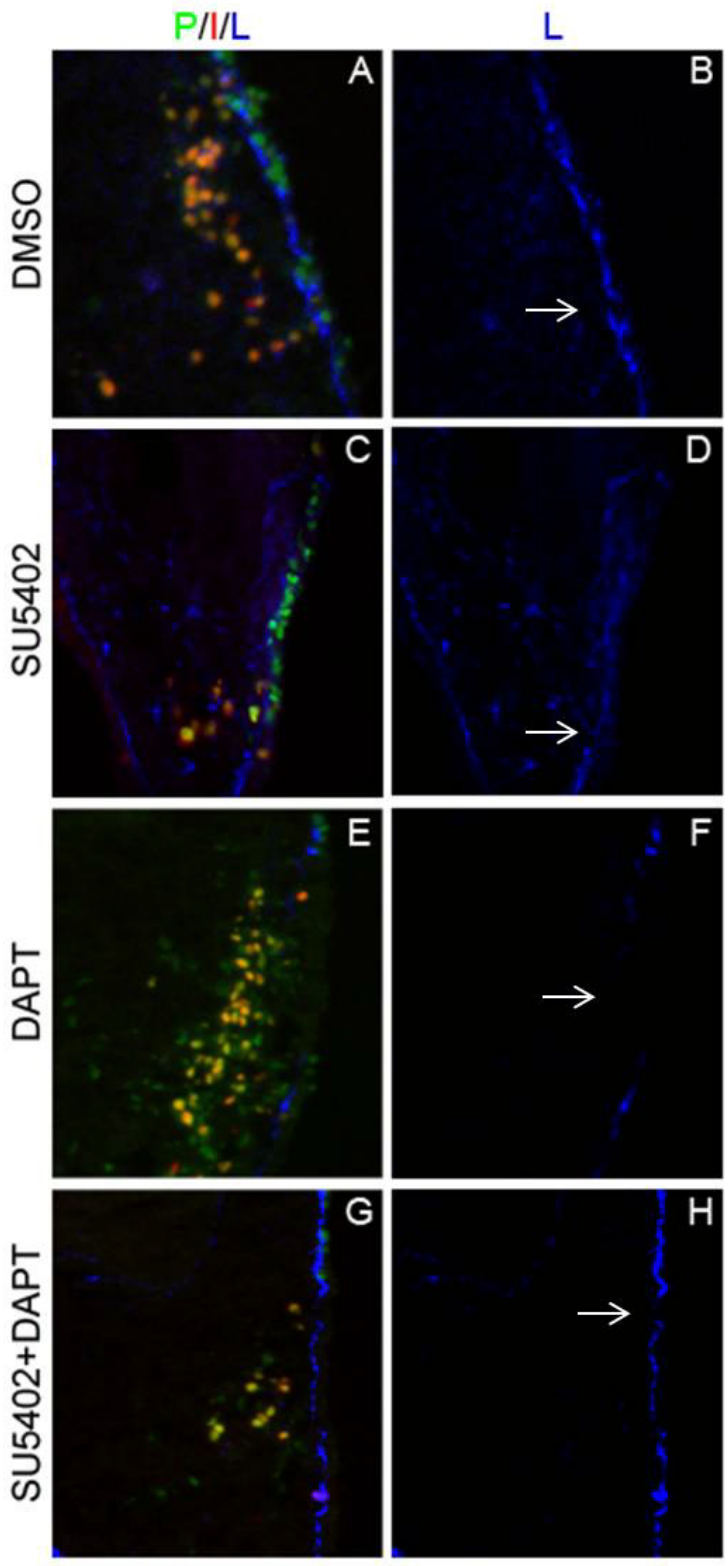

Figure 13 FGF activation coupled with Notch inhibition disrupts basement membrane integrity (legend on page 49)

Figure 13 Transverse sections through the opV placode region of 24-28 ss embryos cultured in DMSO, SU5402, DAPT, or SU5402 plus DAPT for 24 hr in agar-albumin culture dishes. Embryos were prepared as described, cryosectioned, and immunostained for the opV marker Pax3 (P; green), the early neuronal marker Islet1 (I; red), and Laminin (L; blue). Cells co-expressing Pax3 and Islet1 are depicted in yellow. Laminin staining was disrupted in embryos treated with DAPT (F) resulting in large breaks in the basement membrane in the opV region when compared to DMSO controls (B). Disruptions were also noted in embryos treated with SU5402 (D) and SU5402+DAPT (H) treated embryos, but not to the extent as observed in embryos treated with DAPT. Arrows highlight areas of Laminin disruption.

DISCUSSION

Sensory neuron development is a complicated process involving several signaling pathways. Previous studies have found that Wnt, PDGF, FGF, and Notch are all involved in the process of sensory neurogenesis, but it was still unknown how these pathways interact to drive sensory neuron development. It was hypothesized that FGF and Notch interact in one of three mechanisms. First, FGF activation downregulates Notch to drive neurogenesis. Second, Notch downregulation upregulates FGFR4 expression leading to neurogenesis. Or third, FGF and Notch act in parallel to promote neurogenesis. By using a novel multifactorial approach, the FGF and Notch pathways were manipulated individually and simultaneously to help uncover the steps required to drive an undifferentiated opV placode cell to a proneural cell fate in the condensing opV ganglion.

To test whether FGF activation leads to Notch downregulation, FGF was inhibited by sFGFR4 with concurrent inhibition of Notch by DAPT (Figure 2A). This study showed that misexpression the FGF inhibitor sFGFR4 results in cells remaining in the ectoderm and not expressing the proneural marker Islet1. The use of the FGF receptor antagonist, SU5402, was also employed to globally block FGF signaling with concurrent inhibition of Notch by DAPT. This approach allowed for the evaluation of all potential opV sensory neurons and was not dependent on electroporation efficiency. Further, by utilizing this method, embryos were not subjected to the additional impact of electroporation and it was not necessary to transfer embryos from one culture media to another, thus minimizing the chance of damaging the tissue. These results again showed few cells co-expressing Pax3 and Islet1 in the mesenchyme, confirming that FGF inhibition results in failed neurogenesis, even in the context of Notch inhibition. It was

therefore concluded that in normal sensory neurogenesis, FGF activation does not drive Notch downregulation, and subsequently sensory neuron development. Interestingly, more Pax3+/Islet1+ cells were found in the mesenchyme in SU5402+DAPT treated embryos than in sFGFR4+DAPT treated embryos. This may have been due to a less potent effect of SU5402 than sFGFR4, and it is expected that using an increased concentration of SU5402 would result in even fewer cells migrating into the mesenchyme. It was also observed that while downregulation of FGF and Notch disrupted normal neurogenesis (i.e. few targeted cells in the opV mesenchyme), many Islet1 expressing cells were found in the mesenchyme of the maxillo-mandibular region (mmV) in embryos treated with DAPT alone and in embryos treated with SU5402+ DAPT. This finding is significant because it distinguishes a boundary between the opV and mmV regions when FGF and Notch signaling are downregulated concurrently which suggests two things. First, it suggests Notch signaling plays a role in mmV neuronal differentiation and second, it suggests that the mechanism of neurogenesis in the mmV is likely different from the mechanism of neurogenesis in the opV.

It is important to note that results from FGF misexpression experiments with sFGFR4 and Notch inhibition by DAPT were corroborated by experiments conducted by global FGF inhibition with SU5402 and Notch with DAPT. With the advent of new chemical inhibitors, these results help establish the efficacy of treating with two drugs at once which may have significant impact on future areas of research.

Additional experiments were conducted in order to distinguish between Notch downregulation leading to upregulation of FGFR4 driving neurogenesis and FGF and Notch signaling working in parallel to promote neurogenesis (Figure 2B,C) by assaying FGFR4 mRNA expression after treatment with DAPT for 4 or 12 hr. If Notch downregulation resulted in

transient FGFR4 upregulation, then we would expect to see broad, robust expression of FGFR4 mRNA after DAPT exposure; however, results from these experiments showed that FGFR4 mRNA expression was not upregulated by reduced Notch signaling early or later in neuronal differentiation, indicating that FGF and Notch are likely acting in parallel to promote neurogenesis. This result also suggests that FGF and Notch signaling do not regulate one another in opV placode cells and are each necessary but not sufficient to promote neurogenesis in the ophthalmic trigeminal ganglion. These findings are intriguing because Notch signaling is often viewed as a final regulatory switch (Gibb et al., 2010). The data presented here do not negate the role of Notch signaling as the potential endpoint switch for neurogenesis, but indicates that several pathways work together culminating in sensory neuron differentiation.

As described, this study provides strong support for a parallel relationship between FGF and Notch signaling in regulating sensory neuron formation in the opV placode. Inhibition of FGF alone by misexpression of sFGFR4 or globally with SU5402 impeded cells from delaminating. Similarly, constitutive Notch activation by misexpression of the Notch intracellular domain, NICD, inhibits delamination of cells in the opV placode (Lassiter et al., 2010). Here, it was observed that few cells delaminated when FGF signaling was inhibited, even in the presence of Notch downregulation which results in many cells delaminating when inhibited alone. Therefore, it appears that FGF activation with concurrent Notch downregulation is required for cells in the opV placode to undergo delamination.

Although FGF activation with parallel Notch downregulation may be required for delamination, active FGF signaling may not be required for neuronal differentiation. FGF8 misexpression alone does not lead to increased neuronal differentiation (Lassiter et al., 2009) while treatment with DAPT results in robust neurogenesis. This suggests that FGF signaling

plays a role in delamination while Notch signaling plays a role in both delamination and differentiation. However, it was observed that cells that fail to delaminate due to FGF inhibition also fail to differentiate which indicates that delamination may be required for differentiation.

In order to investigate the observation that DAPT treated embryos resulted in an undefined ectoderm, embryos were treated with DMSO, SU5402, DAPT, and SU5402+DAPT and stained with Pax3, Islet1, and Laminin. While embryos treated with DAPT treatment alone resulted in a widely fragmented Laminin staining, embryos treated with SU5402+DAPT did not. From these results, basement membrane fragmentation due to Notch downregulation was reported for the first time. Because this effect was reversed in embryos treated with SU5402+DAPT, FGF activation along with parallel Notch downregulation is likely required for basement membrane fragmentation.

These exciting discoveries lead to the possibility that a signal downregulating Notch in coordination with activated FGF initiates changes that disrupt extracellular matrix proteins in the basement membrane, leading to fragmentation followed by delamination. Once parallel signaling by FGF and Notch has disrupted the basement membrane, continued quiescent Notch signaling acting in coordination with another signal such as an extracellular basement membrane protein, may then lead to neuronal differentiation (Figure 14). It is known that epithelial-mesenchymal transition (EMT) is often caused by disruption of cell-cell and/or cell-extracellular matrix protein interactions (Radisky 2005), but the mechanisms that carry out this process are still unknown in many tissues. In agreement with the model suggested here, it has recently been shown that mammary epithelial EMT in mouse cells is regulated by extracellular basement membrane proteins where Laminin acts to inhibit EMT while fibronectin promotes it (Chen et al., 2013). A similar mechanism regulating opV neuron differentiation may help explain the observation of

many Islet1+ cells in the ectoderm of DAPT treated embryos. It is possible that once FGF and Notch signaling disrupt extracellular basement membrane proteins leading to basement membrane fragmentation, opV cells in the ectoderm interact prematurely with some signal, possibly an extracellular basement membrane protein, to drive neurogenesis along with Notch downregulation.

Examining the effect of extracellular basement membrane proteins on opV placode cells will be an interesting focus of future research and may help determine if quiescent Notch signaling in opV ectoderm cells along with coordinated extracellular basement membrane protein interactions promotes sensory neuron formation.

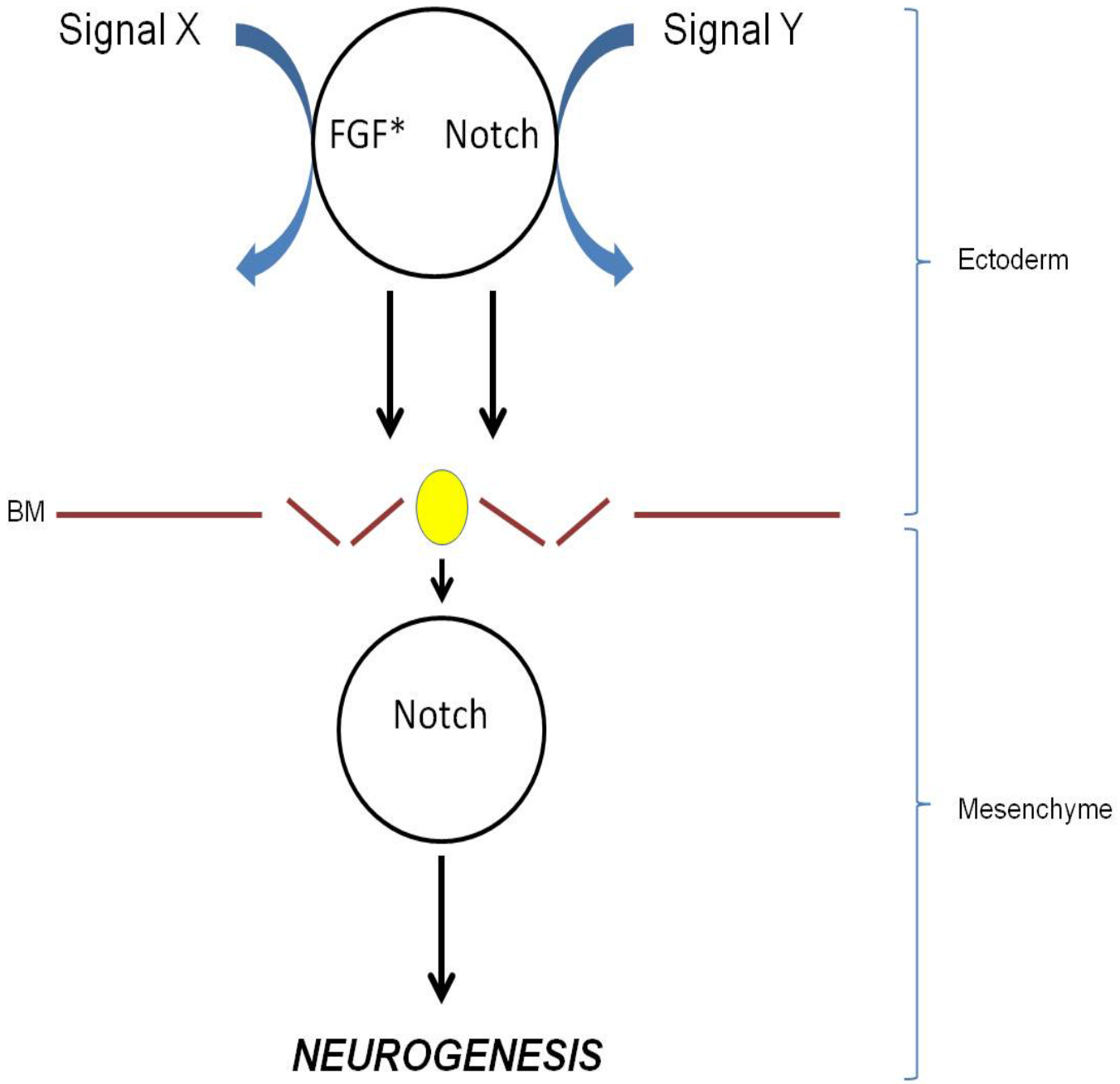

Figure 14 Proposed model for parallel interactions of FGF and Notch signaling leading to neurogenesis in the opV ganglion (legend on page 55)

Figure 14 Parallel activation of FGF and downregulation of Notch leads to disruption of extracellular matrix proteins in the basement membrane leading to fragmentation, delamination, and later, neuronal differentiation by Notch downregulation and cell interaction with an extracellular basement membrane protein.
(Signal X) Unknown signal leading to increased FGF signaling
(Signal Y) Unknown signal leading to downregulation of Notch signaling
(FGF*) Activate FGF signaling
(Notch) Indicates downregulated Notch
(BM) Basement Membrane
Extracellular basement membrane protein

REFERENCES

Abelló, G., Khatri, S., Giráldez, F., Alsina, B., 2007. Early regionalization of the otic placode and its regulation by the notch signaling pathway. Mechanisms of Development 124, 631-645.

Aulehla, A., Wehrle, C., Brand-Saveri, B., Kemler, R., Gossler, A., Kanzler, B., Herrmann, B.G., 2003.Wnt3a plays a major role in the segmentation clock controlling somitogenesis. Developmental Cell 4, 395–406.

Austin, C.P., Feldman, D.E., Ida, Jr., J.A., Cepko, C.L., 1995. Vertebrate retinal ganglion cells are selected from competent progenitors by the actin of Notch. Development 12, 3637-3650.

Baker, C.V., Bronner-Fraser, M., 2000. Establishing neuronal identity in vertebrate neurogenic placodes. Development 127, 3045-56.

Baker, C.V., Bronner-Fraser, M., 2001. Vertebrate cranial placodes I. Embryonic induction. Developmental Biology 232, 1-61.

Baker, C.V., Stark, M.R., Bronner-Fraser, M., 2002. Pax3-expressing trigeminal placode cells can localize to trunk neural crest sites but are committed to a cutaneous sensory neuron fate. Developmental Biology 249, 219-236.

Begbie, J., Ballivet, M., Graham, A., 2002. Early steps in the production of sensory neurons by the nueorgenic placodes. Molecular and Cellular Neuroscience 21, 502-511.

Bolós, V., Grego-Bessa, J., de la Pompa, J.L., 2007. Notch signaling in development and cancer. Endocrine Review 28, 339-363.

Borello, U., Cobos, I., Long, J.E., McWhirter, J.R., Murre, C., Rubenstein, J.L., 2008. FGF15 promotes neurogenesis and opposes FGF8 function during neocortical development. Neural Development 3, 17.

Canning, C.A., Lee, L., Luo, S.X., Graham, A., Jones, C.M., 2008. Neural tube derived Wnt signals cooperate with FGF signaling in the formation and differentiation of the trigeminal placodes. Neural Development 3,35.

Castro, D.S., Skowronska-Krawczyk, D., Armant, O., Donaldson, I.J., Parras, C., Hunt, C., Critchley, J.A., Nguyen, L., Gossler, A., Gottgens, B., Matter, J.M., Guillemot F., 2006. Proneural bHLH and Brn proteins coregulate a neurogenic program through cooperative binding to a conserved DNA motif. Developmental Cell 11, 831-844.

Chapman, S.C., Collingnon, J., Schoenwolf, G.C., Lumsden, A., 2001. Improved Method for Chick Whole-Embryo Culture Using a Filter Paper Carrier. Developmental Dynamics 220, 284-289.

Chen, Q.K., Lee, K., Radisky, D. C., Nelson, C. M., 2013. Extracellular matrix proteins regulate epithelial-mesenchymal transition in mammary epithelial cells.

Chitnis, A., Henrique, D., Lewis, J., Ish-Horowicz, D., Kitner, C., 1995. Primary neurogenesis in *Xenopus* embryos regulated by a homologue of the *Drosophila* neurogenic gene Delta. Nature 375, 761-766.

Chitnis, A., Kitner, C., 1996. Sensitivity of proneural genes to lateral inhibition affects the pattern of primary neurons in *Xenopus* embryos. Development 122, 2295-2301.

Cholfin, J.A., Rubenstein, J.L., 2007. Patterning of frontal cortex subdivisions by Fgf17. Proceedings of the National Academy of Sciences of the United States of America 104, 7652-7657.

D'Amico-Martel, A., Noden, D.M., 1983. Contributions of placodal and neural crest cells to avian cranial and peripheral ganglia. American Journal of Anatomy 166, 445-468.

Darnell, D.K., Schoenwolf, G.C., 2000. Culture of avian embryos. Methods in Molecular Biology 135: 31-37.

Daudet, N., Ariza-McNaughton, L., Lewis, J., 2007. Notch signalling is needed to maintain, but not initiate the formation of prosensory patches in the chick inner ear. Development 134, 2369-2378.

Domínguez-Frutos, E., Vendrell, V., Alvarez, Y., Zelarayan, L.C., López-Hernández, I., Ros, M., Schimmang, T., 2009. Tissue-specific requirements for FGF8 during early inner ear development. Mechanisms of Development 126, 873-81.

Dorsky, R.I., Rapaport, D.H., Harris, W.A., 1995. Notch inhibits cell differentiation in the *Xenopus* retina. Nature 385, 67-70.

Dude, C.M., Kuan, C.Y., Bradshaw, J.R., Greene, N.D., Relaix, F., Stark, M.R., Baker CV. 2009. Activation of Pax3 target genes is necessary but not sufficient for neurogenesis in the ophthalmic trigeminal placode. Developmental Biology 326, 314-26.

Faux, C.H., Turnley, A.M., Epa, R., Cappai, R., Bartlett, P.F., 2001. Interactions between Fibroblast Growth Factors and Notch Regulate Neuronal Differentiation. The Journal of Neuroscience 21, 5587-5596.

Ferjentsik, Z., Hayashi, S., Dale, J.K., Bessho, Y., Herreman, A., De Strooper, B., Monte, G., Pompa, J.L., Maroto, M., 2009. Notch is a critical component of the mouse somitogenesis oscillator and is essential for the formation of the somites. PLOS Genetics 5, e1000662.

Fukuchi-Shimogori, T., Grove, E.A., 2001. Neocortex patterning by the secreted signaling molecule FGF8. Science 294, 1071-1074.

Freter, S., Muta, Y., Mak, S.S., Rinkwitz, S., Ladher, R.K., 2008. Progressive restriction of otic fate: the role of FGF and Wnt in resolving inner ear potential. Development 135, 3415-24.

Garcia, C.M., Huang, J., Madakashira, B.P., Liu, Y., Rajagopal, R., Dattilo, L., Robinson, M.L., Beebe, D.C., 2011. The function of FGF signaling in the lens placode. Developmental Biology 351, 176-85.

Garel, S., Huffman, K.J., Rubenstein, J.L., 2003. Molecular regionalization of neocortex is disrupted in Fgf8 hypomorphic mutants. Development 130, 1903-1914.

Gibb, S., Zagorska, A., Melton, K., Tenin, G., Vacca, I., Trainor, P., Maroto, M., Dale, J.K., 2009. Interfering with Wnt signalling alters the periodicity of the segmentation clock. Developmental Biology 330, 21–31.

Gibb, S., Maroto, M., Dale, J.K., 2010. The segmentation clock mechanism moves up a notch. Trends in Cell Biology 20, 593-600.

Goldbeter, A., Pourquie, O., 2007. Modeling the segmentation clock as a network of coupled oscillations in the Notch, Wnt and FGF signaling pathways. Journal of Theoretical Biology 252, 574-585.

Hébert, J.M., Fishell, G., 2008. The genetics of early telencephalon patterning: some assembly required. Nature Reviews Neuroscience 9, 678-685.

Henrique, D., Adam, J., Myat, A., Chitnis, A., Lewis, J., Ish-Horowicz, D., 1995. Expression of a Delta homologue in prospective neurons in the chick. Nature 375, 787-790.

Hofmann, M., Schuster-Gossler, K., Watabe-Rudolph, M., Aulehla, A., Herrmann, B.G., Gossler, A., 2004. WNT signaling, in synergy with T/TBX6, controls Notch signaling by regulating Dll1 expression in the presomitic mesoderm of mouse embryos. Genes and Development 18, 2712–2717.

Kageyama, R., Ohtsuka, T., Hatakeyama, J., Ohsawa, R., 2005. Roles of bHLH genes in neural stem cell differentiation. Experimental Cell Research 306, 343-348.

Kapsimali, M., Kaushik, A.L., Gibon, G., Dirian, L., Ernest, S., Rosa, F.M., 2011. Fgf signaling controls pharyngeal taste bud formation through miR-200 and Delta-Notch activity. Development 138, 3473-84.

Kiernan, A.E., Ahituv, N., Fuchs. H., Balling, R., Avraham, K.B., Steel, K.P., Hrabé de Angelis, M., 2001. The Notch ligand Jagged1 is required for inner ear sensory development.

Proceedings of the National Academy of Sciences of the United States of America 98, 3873-8.

Ladher, R.K., Church, V.L., Allen, S., Robson, L., Abdelfattah, A., Brown, N.A., Hattersley, G., Rosen, V., Luyten, F.P., Dale, L., Francis-West, P.H., 2000. Cloning and expression of the Wnt antagonist Sfrp-2 and Frzb during chick development. Developmental Biology 218, 183-198.

Ladher, R.K., Wright, T.J., Moon, A.M., Mansour, S.L., Schoenwolf, G.C., 2005. FGF8 initiates inner ear induction in chick and mouse. Genes and Development 19, 603-613.

Ladher, R.K., O'Neill, P., Begbie, J., 2010. From shared lineage to distinct functions: the development of the inner ear and epibranchial placodes. Development 137, 1777-85.

Lanford, P.J., Lan, Y., Jiang, R., Lindsell, C., Weinmaster, G., Gridley, T., Kelley, M.W., 1999. Notch signaling pathway mediates hair cell development in mammalian cochlea. Nature Genetics 21, 289-92.

Lassiter, R.N.T., Dude, C.M., Reynolds, S.B., Winters, N.I., Baker, C.V., Stark, M.R., 2007. Canonical Wnt signaling is required for ophthalmic trigeminal placode cell fate determination and maintenance. Developmental Biology 308, 392-406.

Lassiter, R.N.T., Reynolds, S.B., Marin, K.D., Mayo, T.F., Stark, M.R., 2009. FGF signaling is essential for ophthalmic trigeminal placode cell delamination and differentiation. Developmental Dynamics 238, 1073-1082.

Lassiter, R.N.T., Ball, M.K., Adams, J.S., Wright, B.T., Stark, M.R., 2010. Sensory neuron differentiation is regulated by notch signaling in the trigeminal placode. Developmental Biology 334, 836-848.

Lewis, J., 1998. Notch signalling and the control of cell fate choices in vertebrates. Seminars in Cell and Developmental Biology 9, 583–589.

Léger, S., Brand, M., 2002. Fgf8 and Fgf3 are required for zebrafish ear placode induction, maintenance and inner ear patterning. Mechanisms of Development 119, 91-108.

Lewis, J., Hanisch, A., Holder, M., 2009. Notch signaling, the segmentation clock, and the patterning of vertebrate somites. Journal of Biology 8, 44.

Kawamura, A., Koshida, S., Hijikata, H., Sakaquchi, T., Kondoh, H., Takada, S., 2005. Zebrafish Hairy/Enhancer of split protein links FGF signaling to cyclic gene expression in the periodic segmentation of somites. Genes and Development 19, 1156–1161.

Marcelle, C., Eichmann, A., Halevy, O., Breant, C., Le Douarin, N.M., 1994. Distinct developmental expression of a new avian fibroblast growth factor receptor. Development 120, 683-694.

Martin, K., Groves, A.K., 2006. Competence of cranial ectoderm to respond to Fgf signaling suggest a two-step model of otic placode induction. Development 133, 877-887.

Megason, S.G., McMahon, A.P., 2002. A mitogen gradient of dorsal midline Wnts organize growth in CNS. Development 129, 2087-2098.

Nakamura, H., Katahira, T., Sato, T., Watanabe, Y., Funahashi, J., 2000. Gainand loss of function in chick embryos by electroporation. Mechanisms of Development 121,1137-1143.

Nakaya, Y., Sheng, G., 2009. An amicable separation; Chick's way of doing EMT. Cell Adhesion & Migration 3:2, 160-163.

Nelson, B.R., Hartman, B.H., Georgie, S.A., Lan, M.S., Reh, T.A., 2007. Transient inactivation of Notch signaling synchronizes differentiation of neural progenitor cells. Developmental Biology 304, 479-498.

O'Leary, D.D., Nakagawa, Y., 2002. Patterning centers, regulatory genes and extrinsic mechanisms controlling arealization of the neocortex. Current Opinion in Neurobiology 12, 14-25.

Ohyama, T., Mohamed, O.A., Taketo, M.M., Dufort, D., Groves, A.K., 2006. Wnt signals mediate a fate decision between otic placode and epidermis. Development 133, 865-857.

Ozbudak, E.M., Pourquie, O., 2008. The vertebrate segmentation clock: the tip of the iceberg. Current Opinion in Genetics and Development 18: 317–323.

Raballo, R., Rhee, J., Lyn-Cook, R., Leckman, J.F., Schwartz, M.L., Vaccarino, F.M., 2000. Basic Fibroblast Growth Factor (Fgf2) is necessary for cell proliferation and neurogenesis in the developing cerebral cortex. Journal of Neuroscience 20, 5012-5023.

Radisky, D.C., 2005. Epithelial-mesenchymal transition. Journal of Cell Science 118, 4325-4326.

Rash, B.G., Lim, H.D., Breuniq, J.J., Vaccarino, F.M., 2011. FGF signaling expands embryonic cortical surface area by regulating Notch-dependent neurogenesis. Journal of Neuroscience 31, 15604-17.

Scaal, M., Gros, J., Lesbros, C., Marcell, C., 2004. In ovo electroporation of avian somites. Developmental Dynamics 229, 643-650.

Schimmang, T., 2007. Expression and functions of FGF ligands during early otic development. International Journal of Developmental Biology 51, 473-81.

Schlosser, G., 2006. Induction and specification of cranial placodes. Developmental Biology 294, 303-351.

Shimojo, H., Ohtsuka, T., Kageyama, R., 2008. Oscillations in Notch signaling regulate maintenance of neural progenitors. Neuron 58, 52-64.

Shin, D.M., Korada, S., Raballo, R., Shashikant, C.S., Simeone, A., Taylor, J.R., Vaccarino, F., 2004. Loss of glutamatergic pyramidal neurons in frontal and temporal cortex resulting from attenuating of FGFR1 signaling is associated with spontaneous hyperactivity in mice. Journal of Neuroscience 24, 2247-2258.

Small, D., Kovalenko, D., Soldi, R., Mandinova, A., Kolev, V., Trifonava, R., Bagala, C., Kacer, D., Battelli, C., Liaw, L., Prudovsky, I., Maciag, T., 2003. Notch activation suppresses fibroblast growth factor-dependent cellular transformation. The Journal of Biological Chemistry 278, 16405-16413.

Stark, M.R., Sechrist, J., Bonner-Fraser, M., Marcelle, C., 1997. Neural tube ectoderm interactions are required for trigeminal placode formation. Development 124, 4287-4295.

Stark, M.R., Briggs, J.J., Schoenwolf, G.C., Rao, M.S., 2000. Characterization of avian frizzled genes in cranial placode development. Mechanisms of Development 93, 195-200.

Storm, E.E., Rubenstein, J.L., Martin, G.R., 2003. Dosage of Fgf8 determines whether cell survival is positively or negatively regulated in the developing forebrain. Proceedings of the National Academy of Science of the United States of America 100, 1757-1762.

Sun, Y., Dykes, I.M., Liang, X., Eng, S.R., Evans, S.M., Turner, E.E., 2008. A central role for Islet1 in sensory neuron development linking sensory and spinal gene regulatory programs. Nature Neuroscience 11, 1283-1293.

Vaccarino, F.M., Schwartz, M.L., Raballo, R., Nilsen, J., Rhee, J., Zhou, M., Doetschman, T., Coffin, J.D., Wyland, J.J., Hung, Y.T., 1999. Changes in cerebral cortex size are governed by fibroblast growth factor during embryogenesis. Nature Neuroscience 2, 246-253.

Wahl, M.B., Deng, C., Lewandoski, M., Porquie, O.M.B., 2007. FGF signaling acts upstream of the NOTCH and WNT signaling pathways to control segmentation clock oscillations in mouse somitogenesis. Development 134, 4033–4041.

Wakamatsu, Y., Maynard, T.M., Weston, J.A., 2000. Fate determination of neural crest cells by NOTCH- mediated lateral inhibition and asymmetrical cell division during gangliogenesis. Development 127, 2811-2821.

Xu, H., Dude, C.M., Baker, C.V., 2008. Fine-grained fate maps for the ophthalmic and maxillomandibular trigeminal placodes in the chick embryo. Developmental Biology 317, 174-186.

Yoon, K., Gaiano, N., 2006. Notch signaling in the mammalian central nervous system: insights from mouse mutants. Nature Neuroscience 8, 709-715.

Zine, A., Van De Water, T.R., de Ribaupierre, F., 2000. Notch signaling regulates the pattern of auditory hair cell differentiation in mammals. Development 127, 3373-83.

APPENDIX

Table 7 Cell counts of electroporated embryos with pCIG or sFGFR4 cultured in DMSO and DAPT

pCIG+DMSO

8 embryos	12 placodes	Ectoderm						Mesenchyme					
		Pax3	GFP	Pax3/GFP	Untargeted GFP	Islet1	GFP/Islet1	Pax3	GFP	Pax3/GFP	Untargeted GFP	Islet1	GFP/Islet1
Embryo_A	Section												
1	54	17	16	9	7	1	0	3	2	2	0	18	2
2	58	18	12	9	3	5	1	7	6	3	3	19	2
3	62	22	5	5	0	7	1	5	5	1	4	19	1
4	66	12	4	2	2	2	0	6	4	2	2	22	2
5	69	21	10	10	0	2	0	6	4	2	2	37	2
Total cells		90	47	35	12	17	2	27	21	10	11	115	9
Embryos_B1													
1	128	15	42	11	27	2	1	10	7	4	3	14	4
2	131	7	30	7	23	1	1	9	12	4	8	3	2
Total cells		22	72	18	50	3	2	19	19	8	11	17	6
1	40	13	15	4	11	7	2	8	4	4	0	9	4
2	43	3	13	2	11	0	0	8	9	7	2	12	6
3	46	4	20	1	19	2	0	7	9	5	4	10	4
4	53	10	9	6	3	0	0	4	3	1	2	11	1
Total cells		30	57	13	44	9	2	27	25	17	8	42	15
Embryos_B2													
1	61	13	18	11	7	4	1	1	3	1	2	5	1
2	64	15	19	13	6	3	3	3	5	5	0	8	5
3	67	13	18	7	11	4	1	5	3	3	0	5	3
Total cells		41	55	31	24	11	5	9	11	9	2	18	9
Embryo_C													
1	99	15	29	13	16	2	2	11	9	6	3	17	6
2	105	14	15	9	6	1	1	12	11	6	5	17	5
3	108	20	18	16	2	2	1	15	10	8	2	16	8
4	111	22	17	15	2	2	2	8	5	3	2	17	3
5	114	22	10	9	1	2	1	5	7	5	2	13	5
Total cells		93	89	62	27	9	7	51	42	28	14	80	27
Embryo_D													
1	117_1	15	27	15	12	5	3	8	7	4	3	10	4

	2	120_1	9	14	7	7	0	0	10	18	4	14	17	3
	3	123_1	19	25	16	9	3	3	9	8	4	4	19	3
	4	126_1	11	16	6	10	1	1	11	5	3	2	17	3
	5	129_1	12	11	2	9	0	0	7	6	2	4	10	3
Total cells			66	93	46	47	9	7	45	44	17	27	73	16
	1	117_2	19	10	9	1	4	3	6	4	3	1	17	3
	2	120_2	23	5	5	0	2	0	6	2	2	0	15	2
	3	123_2	14	9	7	2	0	0	7	3	3	0	13	3
	4	126_2	14	11	8	3	2	0	7	0	0	0	10	0
	5	129_2	4	10	3	7	3	0	5	4	2	2	6	2
Total cells			74	45	32	13	11	3	31	13	10	3	61	10
Embryo_E														
	1	148_1	10	21	8	13	0	0	3	5	2	3	8	2
	2	151_1	12	21	12	9	0	0	6	8	4	4	9	4
	3	154_1	15	21	11	10	0	0	4	4	4	0	5	4
	4	157_1	22	17	16	1	1	0	3	5	3	2	4	3
	5	161_1	5	15	4	11	2	1	2	2	2	0	5	2
Total cells			64	95	51	44	3	1	18	24	15	9	31	15
	1	148_2	14	24	11	13	0	0	3	3	3	0	3	2
	2	151_2	16	26	13	13	0	0	4	3	2	1	5	2
	3	154_2	19	19	12	7	1	0	4	7	3	4	5	3
	4	157_2	14	19	13	6	1	1	3	4	2	2	5	2
	5	161_2	7	18	6	12	0	0	3	4	3	1	4	3
Total cells			70	106	55	51	2	1	17	21	13	8	22	12
Embryo_F														
	1	57	27	29	26	3	2	2	9	10	9	1	25	8
	2	61	29	32	26	6	0	0	7	8	6	2	11	6
	3	64	17	15	13	2	2	2	5	7	4	3	11	4
	4	67	13	9	7	2	1	0	6	6	5	1	10	5
Total cells			86	85	72	13	5	4	27	31	24	7	57	23
	1	72	24	15	15	0	3	2	6	7	4	3	10	4
	2	73	15	30	15	15	0	0	7	7	5	2	12	5
	3	76	19	33	17	16	0	0	1	3	1	2	6	1
	4	82	19	20	15	5	8	8	7	8	6	2	9	6
Total cells			77	98	62	36	11	10	21	25	16	9	37	16
Embryo_G														
	1	85	9	9	7	2	1	0	4	5	3	2	6	3
	2	88	5	7	3	4	0	0	8	2	2	0	7	2
Total cells			14	16	10	6	1	0	12	7	5	2	13	5

sFGFR4+DMSO

6 embryos	7 placodes	Ectoderm			Mesenchyme		
		GFP	Islet1	GFP/Islet1	GFP	Islet1	GFP/Islet1
Embryo_11	section						
1	1	36	0	0	0	0	0
2	3	27	0	0	0	0	0
3	4	26	0	0	0	0	0
4	5	33	0	0	0	1	0
5	6	38	0	0	0	0	0
Total Cells		196	0	0	0	1	0
Embryo_FGF2							
1	1	21	0	0	1	0	0
2	2	17	1	1	1	0	0
3	3	15	0	0	3	1	0
Total Cells		53	1	1	5	1	0
Embryo_FGF1							
1	1	43	9	9	1	0	0
2	2	41	7	7	0	0	0
3	3	36	0	0	0	0	0
4	4	57	0	0	4	0	0
5	5	49	0	0	4	0	0
Total Cells		226	16	16	9	0	0
Embryo_FGF3							
1	1	19	0	0	0	0	0
2	2	17	0	0	0	0	0
3	3	21	0	0	0	0	0
4	4	14	0	0	0	0	0
5	5	22	0	0	0	0	0
Total Cells		93	0	0	0	0	0
Embryo_FGF4							
1	6	19	0	0	0	2	0
2	7	31	0	0	0	0	0
3	8	21	0	0	0	0	0
4	9	27	0	0	0	0	0
5	10	17	0	0	0	0	0
Total Cells		115	0	0	0	2	0

Embryo_FGF6							
1	3	26	0	0	0	0	0
2	4	21	0	0	0	0	0
3	5	16	0	0	0	0	0
4	6	19	0	0	0	0	0
5	7	12	0	0	0	0	0
Total Cells		94	0	0	0	0	0
1	3	26	0	0	0	0	0
2	4	13	0	0	0	0	0
3	5	16	0	0	0	0	0
4	6	11	0	0	0	0	0
5	7	14	0	0	0	0	0
Total Cells		80	0	0	0	0	0

pCIG+DAPT

10 embryos	17 placodes	Ectoderm			Mesenchyme		
		GFP	Islet1	GFP/Islet1	GFP	Islet1	GFP/Islet1
Embryo_A							
1	35	24	0	0	5	8	3
2	40	10	0	0	11	27	3
3	44	25	0	0	4	70	2
Total cells		59	0	0	20	105	8
1	51	19	6	1	15	42	7
2	54	15	3	0	16	41	5
3	59	11	3	0	9	37	7
4	64	14	6	0	15	35	5
5	75	21	3	0	10	19	4
Total cells		80	21	1	65	174	28
Embryo_B							
1	72	25	0	0	3	38	1
2	77	17	6	0	3	52	1
3	80	22	5	0	3	65	3
Total cells		64	11	0	9	155	5
1	104	38	6	4	18	79	2
2	110	31	2	0	18	60	2
3	113	44	24	2	8	33	2
4	116	29	7	2	13	49	2
5	144	26	4	4	31	55	18

Total cells		168	43	12	88	276	26
Embryo_C							
1	156	33	5	4	57	115	35
2	159	18	5	5	81	138	32
3	162	14	2	1	65	145	21
4	165	15	3	3	45	129	25
Total cells		80	15	13	248	527	113
1	159	33	9	5	22	16	5
2	165	28	3	3	22	17	7
3	162	20	1	1	14	24	4
Total cells		81	13	9	58	57	16
Embryo_D							
1	61	28	5	2	11	17	7
2	64	22	3	3	10	17	5
3	69	16	2	2	18	21	5
4	72	17	8	7	17	18	7
5	76	14	2	2	13	15	8
Total cells		97	20	16	69	88	32
1	64	32	3	2	7	11	2
2	69	22	2	1	21	29	11
3	72	26	9	7	19	33	12
4	76	24	4	2	18	24	10
5	80	18	12	4	18	22	10
Total cells		122	30	16	83	119	45
Embryo_E							
1	86	25	11	7	23	64	13
2	89	28	10	5	32	74	8
3	92	16	7	3	15	76	6
4	95	30	7	4	19	40	14
5	98	15	1	0	23	59	9
Total cells		114	36	19	112	313	50
	102	3	7	0	6	31	6
	105	2	6	0	9	40	7
	108	5	10	0	10	45	9
	114	2	14	1	11	65	8
	117	32	9	3	9	29	4
Total cells		44	46	4	45	210	34

Embryo_F							
1	120	34	7	0	8	34	4
2	123	36	15	6	14	56	8
3	126	29	17	6	11	67	6
4	129	31	12	3	8	64	3
Total cells		130	51	15	41	221	21
Embryo_G							
1	1	7	5	1	7	27	5
2	7	5	8	3	9	81	5
3	17	10	3	0	21	90	2
4	23	22	5	2	30	101	10
Total cells		44	21	6	67	299	22
1	7	10	0	0	9	19	8
2	10	18	2	2	7	26	5
3	17	22	2	2	19	35	7
4	23	14	4	4	21	54	7
Total cells		64	8	8	56	134	27
Embryo_H							
1	26	0	4	0	16	87	9
2	30	6	4	0	13	75	10
3	33	14	6	1	16	75	11
4	37	20	4	0	14	67	10
5	44	4	2	0	20	62	9
Total cells		44	20	1	79	366	49
1	30	22	14	5	4	8	2
2	33	17	15	8	5	8	3
3	37	19	12	4	4	17	3
4	44	20	6	2	21	26	8
Total cells		78	47	19	34	59	16
Embryo_G2	2	13	7	0	15	37	10
	3	12	10	0	9	51	8
	4	8	20	3	10	69	8
	5	4	31	3	12	78	12
	9	5	28	5	8	87	8
Total Cells		42	96	11	54	322	46
Embryo_A2	1	8	35	8	10	46	8

	2	5	28	5	17	35	13
	3	4	11	4	16	36	13
	4	9	13	1	7	31	5
	5	2	2	0	4	12	4
Total Cells		28	89	18	54	160	43

sFGFR4+DAPT

10 embryos	17 placodes	Ectoderm			Mesenchyme		
		GFP	Islet1	GFP/Islet1	GFP	Islet1	GFP/Islet1
Embryo_D							
1	1	33	12	0	2	25	0
2	2	27	20	0	3	57	0
3	3	38	26	1	0	70	0
4	5	42	25	0	1	67	0
5	8	46	33	0	8	61	0
Total Cells		186	116	1	14	280	0
Embryo_E							
1	1	23	35	0	3	107	0
2	2	21	31	1	2	138	1
3	3	13	63	0	2	122	0
4	4	18	37	0	1	90	0
5	5	18	36	0	2	88	1
Total Cells		93	202	1	10	545	2
1	1	18	2	0	0	29	0
2	3	20	11	0	0	61	0
3	4	24	25	0	0	42	0
4	5	23	35	1	3	30	0
5	6	25	26	0	1	65	0
Total Cells		110	99	1	4	227	0
Embryo_F							
1	2	11	11	0	1	72	0
2	3	12	12	0	3	50	0
3	4	13	9	0	1	44	0
4	5	20	3	0	0	31	0
5	6	18	12	0	3	45	0
Total Cells		74	47	0	8	242	0
Embryo_P							

1	8	16	13	1	2	61	1
2	12	16	20	0	1	90	1
3	14	21	9	0	0	69	0
4	16	17	5	1	6	65	0
5	18	12	0	0	0	30	0
Total Cells		82	47	2	9	315	2
Embryo_5							
1	1	29	18	0	4	35	0
2	2	53	9	1	1	36	0
3	3	36	14	1	2	27	1
4	4	53	9	0	0	18	0
5	5	38	9	1	0	12	0
Total Cells		209	59	3	7	128	1
Embryo_6							
1	6	8	4	0	0	23	0
2	7	13	19	1	2	25	0
3	9	19	30	0	2	23	2
4	11	13	22	0	4	30	3
5	12	15	19	0	4	24	2
Total Cells		68	94	1	12	125	7
Embryo_9							
1	1	39	32	3	0	30	0
2	3	33	22	1	4	36	0
3	4	48	19	1	1	17	0
4	5	28	20	1	3	27	0
5	6	25	14	0	2	20	0
Total Cells		173	107	6	10	130	0

Table 8 Cell counts of embryos cultured in DMSO, SU5402, DAPT, or SU5402+DAPT

DMSO

3 embryos	4 placodes	Ectoderm			Mesenchyme		
		Pax3	Islet1	Pax3/Islet1	Pax3	Islet1	Pax3/Islet1
Embryo_F							
1	10	20	0	1	16	9	9
2	12	6	0	0	10	3	3
3	13	5	0	0	11	4	4
4	14	4	0	0	12	6	6
5	15	4	2	1	6	3	3
Total Cells		39	2	2	55	25	25
Embryo_G							
1	2	29	0	2	13	21	21
2	3	28	4	5	26	30	29
3	4	31	4	7	22	21	20
4	7	11	0	2	23	12	12
5	9	4	0	2	33	9	9
Total Cells		103	8	18	117	93	91
1	2	34	3	3	19	23	23
2	5	35	3	2	11	21	18
3	7	22	3	0	16	28	28
4	8	7	1	2	18	33	32
5	11	5	4	0	22	24	22
Total Cells		103	14	7	86	129	123
Embryo_H							
1	12	9	0	6	6	22	18
2	13	15	3	1	10	34	32
3	14	21	3	3	20	30	27
4	15	24	1	7	15	18	18
5	16	27	0	7	9	11	8
Total Cells		96	7	24	60	115	103

SU5402

2 embryos	4 placodes	Ectoderm			Mesenchyme		
		Pax3	Islet1	Pax3/Islet1	Pax3	Islet1	Pax3/Islet1
Embryo_A							
1	42	14	0	0	16	11	11

2	44	6	0	0	16	16	16
3	46	7	3	3	13	14	14
4	51	9	3	3	10	9	9
5	52	6	2	2	6	8	8
Total Cells		42	8	8	61	58	58
1	41	7	2	1	19	11	11
2	44	12	4	4	8	10	10
3	45	12	1	1	6	5	5
4	47	6	4	4	11	12	11
5	49	1	0	0	6	7	7
Total Cells		38	11	10	50	45	44
Embryo_D							
1	36	21	0	0	11	15	12
2	40	7	0	0	10	5	4
3	41	14	0	0	7	7	6
4	46	21	1	1	5	9	9
5	48	12	2	2	4	4	4
Total Cells		75	3	3	37	40	35
1	37	7	1	0	3	9	7
2	38	14	0	0	2	5	5
3	39	5	2	2	11	5	5
4	40	15	2	0	6	8	6
5	42	5	2	2	5	10	7
Total Cells		46	7	4	27	37	30

DAPT

1 embryos	2 placodes	Ectoderm			Mesenchyme		
		Pax3	Islet1	Pax3/Islet1	Pax3	Islet1	Pax3/Islet1
Embryo_A							
1	4	23	47	23	47	76	47
2	6	9	46	9	23	57	23
3	7	14	37	14	29	48	29
4	8	3	29	3	33	49	33
5	9	2	34	2	26	46	26
Total Cells		51	193	51	158	276	158
1	9	6	10	6	35	93	35
2	5	16	10	10	102	108	102

3	6	24	4	4	70	93	69
4	7	9	4	4	66	115	61
5	8	12	10	10	46	80	46
Total Cells		67	38	34	319	489	313

SU5402+DAPT

3 embryos	5 placodes	Ectoderm			Mesenchyme		
		Pax3	Islet1	Pax3/Islet1	Pax3	Islet1	Pax3/Islet1
Embryo_F							
1	35	15	6	5	14	17	16
2	37	16	6	6	18	13	13
3	38	8	0	3	15	15	12
4	39	5	5	5	8	5	5
5	41	15	8	8	7	7	7
Total Cells		59	25	27	62	57	53
1	25	11	6	6	10	8	4
2	26	5	2	2	11	9	2
3	28	12	12	12	21	18	5
4	31	10	2	2	8	8	7
5	33	18	5	5	8	7	2
Total Cells		56	27	27	58	50	20
Embryo_FA							
1	51	23	3	3	13	4	8
2	52	14	1	0	2	3	9
3	54	12	6	5	5	5	17
4	57	3	4	3	8	9	8
5	58	6	5	5	5	2	7
Total Cells		58	19	16	33	23	49
Embryo_G							
1	22	12	1	1	13	13	13
2	23	10	5	5	13	11	11
3	25	18	5	5	11	5	5
4	26	6	5	5	8	7	7
5	27	7	2	2	10	9	9
Total Cells		53	18	18	55	45	45
1	22	23	0	0	16	14	14
2	23	13	0	0	11	11	11

3	24	14	0	0	14	9	9
4	25	12	1	0	8	9	9
5	26	14	2	1	12	10	10
Total Cells		76	3	1	61	53	53

CURRICULUM VITAE

5820 NE 42ND STREET KANSAS CITY, MO 64117

PHONE: 816-294-1447 EMAIL: JACOBVOELKEL@YAHOO.COM

JACOB VOELKEL

EDUCATION

Medical Degree- December 2016 — University of Missouri- Kansas City School of Medicine

Master of Science- August 2013 — Brigham Young University
Physiology and Developmental Biology

Bachelor of Science- April, 2009 — Brigham Young University
Major- Neuroscience
Second Major—Biology

PUBLICATIONS

- "Collision Cross Sectional Areas by Fourier Transform Ion Cyclotron Resonance (CRAFTI): A New Method for Characterizing Molecular Structure." Analytical Chemistry 2011. Fan Yan, Jacob E. Voelkel, and David V. Dearden*
- "Remediation of Heavy Metal Ions in Wastewater by Coffee Grounds," CHE 111 MWSU Laboratory Manual, 2007 ed. Jacob E. Voelkel

POSTER PRESENTATIONS

- American Society of Mass Spectrometry (ASMS) conference, "Cross Sectional Areas by Fourier Transform Ion Cyclotron resonance (CRAFTI): A New Method for Probing Ion Conformation." June 2009
- ASMS, "Selective Supramolecular Nanoboxes: Trapping of Small Molecules by Cucurbit[5]uril and Decamethylcucurbit[5]uril Characterized in the Gas Phase Using FTICR/MS." June 2008
- Undergraduate Research Institute Symposium (URIS), "Remediation of Heavy Metal Ions in Wastewater by Coffee

Grounds." October 2006
- URIS, "Clinical Analysis Project (CAP): An Integrated, Inquiry-centered Laboratory Sequence for CHE 111 General Chemistry." October 2006

TEACHING/WORK EXPERIENCE

August 2010 – April 2011 Brigham Young University

Physiology Lab Instructor- Teaching assistantship

- Lectured ~100 students per semester
- Demonstrated proper lab techniques
- Responsible for preparing grades for more than 200 students

August 2009 – June 2010 Nelson Laboratories

Medical Lab Analyst (Pharmaceutical)

- Conducted GLP, GDP, GTP studies
- Maintained cell cultures
- Analyzed lab results

September 2006 – July 2009 Sprint Nextel

Floor Manager

- Managed and trained 12 employees to reach individual sales goals
- Awarded excellent communication specialist honors
- Achieved National Area top 3 salesman honors- 2006,2008,2009

July 2007 – May 2009 Brigham Young University

Research Assistant

- Developed, conducted, and analyzed research experiments using problem solving skills and FTICR-MS for publication
- Organized and presented data during weekly group meetings

AWARDS

- Research Assistantship, Department of Physiology and Developmental Biology, Brigham Young University, Provo, UT, 2011
- Teaching Assistantship, Department of Physiology and Developmental Biology, Brigham Young University, Provo, UT, 2010

- Research Grant- Office of Research and Creative Activities, Brigham Young University, 2009 ($3000)
- Academic scholarship, Brigham Young University, 2007-2008

OTHER LANGUAGES

- Hungarian